Faculty of Sciences
Department of Chemical and Forensic Sciences

Oxidase-Mimic Activities of Copper-Based Particles for Colorimetric Determination of Chromium (VI)

by

KUDA FEKE
ID No: 19100100
BSc (Chemistry) (UB)

A Thesis Submitted to the Faculty of Sciences in Partial Fulfilment of the Requirements for the Award of the Degree of Master of Science in Chemistry of BIUST

Supervisor(s): Dr. Melisew Tadele Alula
Department of Chemistry
Faculty of Science, BIUST
E-mail Address: alulam@biust.ac.bw

May 2023

TABLE OF CONTENTS

Declaration regarding the work and copyright IV
Certification V
Acknowledgements VI
Dedication VII
List of tables VIII
List of figures IX
Abbreviations IX
List of publications XI
Abstract XII
Chapter 1: Introduction 1
1.1. Heavy metals 1
1.2. Chromium (VI) 1
1.3. Nanomaterials 2
1.4. Nanozymes 3
1.4.1. Peroxidase- mimic activity 3
1.4.2. Oxidase- mimic activity 5
1.4.3. Catalase activity 6
1.4.4. Superoxide dismutase activity 6
1.4.5. Hydrolase 6
1.5. Statement of the problem 7
1.6. Aims and Objectives 7
1.7. Significance of study 7
1.8. Thesis Layout 7
Chapter 2: Literature review 9
2.1. Water pollution 9
2.2. Emerging contaminants 10
2.3. Water status in Botswana 11
2.4. Methods for detection of heavy metals in water 11
2.5. Detection of chromium 12
2.6. Copper- based nanoparticles 13
2.7. Synthesis of copper- based nanoparticles 13

2.7.1. Solvothermal method 14
Chapter 3: Chromium (VI) detection based on the enhanced oxidase- like activity of the recoverable CuS/ Fe_3O_4 composite 15
3.1 Introduction 15
3.2 Experimental 17
3.2.1 Chemicals 17
3.2.2 Instrumentation 17
3.2.3 Preparation of Copper Sulphide 18
3.2.4 Synthesis of CuS/Fe_3O_4 composites 18
3.2.5 Preparation of solutions 18
3.2.6 Synergy effect 19
3.2.7 Enzyme-mimic activity of the CuS/Fe_3O_4 nanocomposites 19
3.2.8 Optimization of parameters 19
3.2.9 Optimization for mass 20
3.2.10 Optimization for pH 20
3.2.11 Optimization for concentration of TMB 20
3.2.12 Colorimetric detection of chromium (VI) 20
3.2.13 Steady state kinetics assay 21
3.2.14 Sensitivity 22
3.2.15 Selectivity 22
3.2.16 Real sample analysis 22
3.3 Results and Discussion 22
3.3.1 Characterization of CuS/Fe_3O_4 22
3.3.2 Catalytic activity of CuS/Fe_3O_4 24
3.3.3 Optimization of the catalytic performance of CuS/Fe_3O_4 in sensing chromium (VI) 27
3.3.4 Steady-state kinetic assay 29
3.3.5 Sensitivity and selectivity of the method 30
3.3.6 Determination of Cr^{6+} in tap water 33
3.4 Summary 34
Chapter 4: Colorimetric detection of chromium (VI) via its instigation of oxidase-mimic activity of CuO 35
4.1. Introduction 35
4.2. Experimental 37
4.2.1. Chemicals 37

4.2.2. Instrumentation 37
4.2.3. Preparation of the copper oxide nanoparticles 38
4.2.4. Preparation of solutions 38
4.2.5. Enzyme-mimic activity of the CuO nanoparticles 38
4.2.6. Optimization of parameters 39
4.2.7. Optimization for mass 39
4.2.8. Optimization for concentration of TMB 39
4.2.9. Optimization for pH 39
4.2.10. Optimization for temperature 39
4.2.11. Colorimetric detection of chromium (VI) 40
4.2.12. Steady state kinetics study 40
4.2.13. Sensitivity 40
4.2.14. Selectivity 40
4.2.15. Real sample analysis 41
4.3. Results and discussion 41
4.3.1. Characterization of CuO 41
4.3.2. Chromium (VI) as an initiator of enzyme-mimic activity of CuO 42
4.3.3. Factors affecting the enzyme-mimic activity of CuO 43
4.3.4. Catalytic reaction mechanism 44
4.3.5. Steady-state kinetic study 45
4.3.6. Sensitivity and selectivity of the method for determining chromium (VI) 45
4.3.7. Analysis of chromium (VI) in tap water 48
4.4. Summary 49
CHAPTER 5: Conclusion 49

DECLARATION REGARDING THE WORK AND COPYRIGHT

Candidate: KUDA FEKE

Student ID: 19100100

Thesis Titled: Oxidase- Mimic Activities of Copper- Based Particles for Colorimetric Determination of Chromium (VI)

I, Kuda Feke, certify that the Thesis is all my own original work and that I have not obtained a degree inthis University or elsewhere on the basis of any of this work.

(If the thesis is based on a group project, then the student must indicate the extent of her / his contribution,with reference to any other theses submitted or published by each collaborator in the project, and a declaration to this effect must be included in the thesis)

This dissertation/thesis is copyright material protected under the Berne Convention, the Copyright and Neighbouring Rights Act, Act. No. 8 of 2000 and other international and national enactments, in that behalf, on intellectual property. It must not be reproduced by any means, in full or in part, except for shortextracts in fair dealing; for researcher private study, critical scholarly review or discourse with an acknowledgement, without the written permission of the office of the Postgraduate School, on behalf of both the author and the BIUST.

Signed:_____ Date:_____25/ 01/ 2023_____

Primary Supervisor (please write in caps or type): MELISEW TADELE ALULA

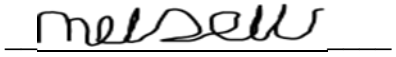
I, the Candidate's **Primary Supervisor**, hereby confirm that I have inspected the above titled thesis and,to the best of my knowledge, it is based on the original work of the candidate.

Signed:_____ Date: _____26 January 2023_____

CERTIFICATION

The undersigned certifies that he has read and hereby recommends for acceptance by the Faculty of Science a dissertation titled: **OXIDASE- MIMIC ACTIVITIES OF COPEER- BASED PARTICLES FOR COLORIMETRIC DETERMINATION OF CHROMIUM (VI)** in fulfilment of the requirements for the degree of Master of Science in Chemistry (MSc Chemistry) of the Botswana International University of Science and Technology.

Approved by:



Dr Melisew Tadele Alula

(Supervisor)

Date: 26 January 2023

ACKNOWLEDGEMENTS

With the help of God, I was able to overcome all the challenges I faced and able to rise through the difficulties.

I also extend my gratitude towards my supervisor Dr. Melisew Tadele Alula for the advice and feedback throughout the course of the project. He was always available to help, patient with me and always willing to shed some light whenever I was lost. I want to also thank my friends for always having my back and my family for believing in me. Special thanks to Tshiamo Frank.

Lastly, I want to thank BIUST for giving me the opportunity to mature as a research scientist and for the funding. I would like to thank Mr. Madiba for his help with XRD analysis and H. Spende, A. Waag and P. Lemmens for their help with SEM and EDX analysis.

DEDICATION

This work is dedicated to me, my supervisor, BIUST, family, friends and above all the one who makes all things possible, Almighty God.

LIST OF TABLES

Table 3.1: Comparison of the CuS/Fe_3O_4 nanocomposites method with other reported peroxidase- like colorimetric methods……...……**30**

Table 3.2: Percentage recoveries for CuS/Fe_3O_4 ……..……**33**

Table 4.1: Comparison of the CuO nanoparticles method with other reported peroxidase- like colorimetric methods…….……....**46**

Table 4.2: Percentage recoveries for CuO NPs …….……...**47**

LIST OF FIGURES

Figure 1.1: (**a**) Michaelis- Menten curve (**b**) Lineweaver- Burk plot……**4**

Figure 1.2: Ping- pong reaction mechanism……...……**5**

Figure 1.3: Ping- pong Lineweaver- Burk plot……..……**5**

Figure 3.1: Characterization of CuS/Fe_3O_4 ……..……**23**

Figure 3.2: Oxidation reaction between TMB and Cr^{6+}……**24**

Figure 3.3: (**a**) UV/ Vis spectra for catalytic activity of CuS/Fe_3O_4 (**b**) UV/ Vis spectra for effect of particles……..……**25**

Figure 3.4: (**a**) Effect of oxygen on oxidation of TMB (**b**) catalytic reaction mechanism of CuS/Fe_3O_4 nanocomposites……...**26**

Figure 3.5: Optimization of (**a**) pH of buffers (**b**) mass of the nanocomposites……...**27**

Figure 3.6: Optimization of concentration of TMB……..**28**

Figure 3.7: Steady state kinetics ……...……...……...….**29**

Figure 3.8: Sensitivity……...**30**

Figure 3.9: Selectivity……...……**31**

Figure 3.10: Real sample analysis……...…….….**32**

Figure 4.1: Characterization of CuO nanoparticles……...…….....**40**

Figure 4.2: (**a**) UV/ Vis spectra for catalytic activity of CuO nanoparticles (**b**) optimization for mass……**41**

Figure 4.3: Optimization for (**a**) pH of buffer (**b**) temperature ……..…...**42**

Figure 4.4: UV/ Vis spectra showing the catalytic reaction mechanism…….……**43**

Figure 4.5: Steady state kinetics…….……...…...**44**

Figure 4.6: Sensitivity and selectivity……...……**45**

Figure 4.7: Bar graph of binary mixtures for selectivity study……**46**

ABBREVIATIONS

EDX- energy dispersive x- ray

LOD- limit of detection

LOQ- limit of quantification

SEM- scanning electron microscopy

TMB- 3, 3', 5, 5', -tetramethylbenzidine

XRD- x-ray diffractometer

ROS- reactive oxygen species

NMs- nanomaterials

LIST OF PUBLICATIONS

1. **Kuda Feke**, Melisew Tadele Alula, Colorimetric detection of chromium (VI) via its instigation of oxidase-mimic activity of CuO, Spectrochimica Acta Part A: Molecular and Biomolecular Spectroscopy, 294, 2023, 122539.
2. **Kuda Feke**, Melisew Tadele Alula, Hendrik Spende, Andreas Waag and Peter Lemmens, Synthesis of a recoverable CuS/ Fe3O4 composite structure with enhanced oxidase-like activity for detection of chromium (VI), Journal of Cluster Science, 34, 2022, 1009-1018.
3. Melisew Tadele Alula and **Kuda Feke**, Peroxidase-like activity of silver nanoparticles loaded filter paper and its potential application for sensing, Journal of Cluster Science, 34, 2021, 613- 621.

ABSTRACT

Extensive use of chromium (VI) in industrial processes such as leather tanning, textile dyeing and metal plating among others has led to it being one of the major pollutants that are discharged to water sources. Chromium (VI) is a toxin with detrimental health effects to mammals. Because of its high toxicity, it is recommended that its concentration in water be limited and therefore organizations such as the World Health Organization (WHO) has set a limit of 0.005 ppm as its maximum level in waste water, the French regulations set its maximum level in drinking water as 0.5 mg/ L and the US Environmental Protection Agency also have a limit of 0.05 mg/ L in drinking water. Techniques have since been developed for detection of Cr (VI) and they include mass spectroscopy, chromatography and also colorimetric methods such as Localized Surface Plasmon Resonance (LSPR) among others but they encounter shortcomings such as complexity, high cost, the need for controlled particle- analyte distance and so on. Therefore herein a hydrothermal method was employed to synthesize copper- based nanoparticles and techniques such as energy dispersive X-ray spectroscopy (EDX), scanning electron microscopy (SEM), transmission electron microscopy (TEM) and X- ray diffraction (XRD) were employed for characterization purposes. The nanoparticles which include CuO and CuS/Fe_3O_4 were found to possess enzyme- mimic activities which can be used for detection of Cr (VI) colorimetrically and hence address the shortcomings of the above mentioned techniques. This technique involves the oxidation of 3, 3', 5, 5'- tetramethylbenzidine (TMB) when introduced to a system containing the nanoparticles and chromium (VI). Chromium (VI) promotes the oxidase-like activity of CuO and CuS/Fe_3O_4 using oxygen as an oxidant such that a deep blue colored 3,3′,5,5′- tetramethylbenzidine diamine (oxTMB) solution was formed by oxidation of a colorless 3, 3', 5, 5'- tetramethylbenzidine (TMB) solution rapidly. The intensities of oxTMB increased proportionally with concentration of chromium (VI) that effects sensitive detection of chromium (VI) by colorimetry. When CuS/Fe_3O_4 nanocomposites are present; with optimum conditions of pH 4.0, 2.5 mg catalyst load and 6 mM concentration of TMB, LoD as low as 0.060 µM and a broad linear range of 0- 1500 µM were obtained. Using CuO as oxidase-like catalyst LoD of 0.079 µM and a linear range of 0.1- 650 µM were acquired using 2.0 mg of the particles, buffer of pH 4.0 and 10 mM of TMB. The methods proved to be selective of chromium (VI) among

other interfering cations and anions. The assays were applied for analysis of chromium (VI) using tap water and proved to be feasible for real sample analysis. These methods proved to be able to address the shortcomings of the above mentioned techniques since they are cheap, rapid and simple compared to the other techniques.

CHAPTER 1: Introduction

1.1. Heavy metals

Heavy metals are metallic chemical elements that are toxic even at low concentrations with density more than 5g/ cm^3. They exist naturally in trace components in the aquatic environment [1]. They include mercury, cadmium, hexavalent chromium, and lead among others. Due to their ability to increase in concentration overtime in a biological organisms, heavy metals are considered significant pollutants [2]. They can make their way to water sources naturally from rocks, veld fires, volcanic activity and breaking down of soil due to acidic rain and because of industrial or consumer waste and agriculture. Their toxicity may cause mutations, lung cancer, damage to essential organs like the liver and kidneys, impairment to the mental and central nervous system [3], [4]. When exposed to heavy metals for a prolonged period diseases such as Alzheimer's, sclerosis, muscular dystrophy and Parkinson's are commonly experienced.

1.2. Chromium (VI)

It is a heavy metal that people are exposed to as a contaminant due to an increase in industries worldwide. Workers are exposed to it through industrial processes like leather tanning, stainless steel production and chrome plating [5]. Exposure to Cr^{6+} leads to allergic dermatitis, chromosomal damages, DNA transformations and mutations in mammalian cells due to it being carcinogenic [6]. This heavy metal is toxic and easily penetrates the mammalian cells in its hexavalent state. Its carcinogenicity can be described using the uptake- reduction method which explains that Cr^{6+} is reduced in cells by cellular reductants to lower oxidation states such as Cr (III), Cr (IV) and Cr (V) which is the most vital step. The cellular reductants include glutathione, ascorbate, microsomes, mitochondria and cells among others. These intermediates therefore lead to DNA strand breaks and mutations [7]. The intermediates are capable of generating free radicals knowns as ROS (reactive oxygen species) that can cause the mutations and DNA breaks [7]. Its toxicity has led to it being recorded as a priority contaminant by the U.S Environmental protection agency [8].

The toxicity and exposure to Cr^{6+} has led to an interest in developing highly selective and sensitive methods for its detection to reduce its consumption by humans and animals. Sensitive methods such as atomic absorption spectroscopy [9], ion chromatography [10], mass spectroscopy [11] and Raman spectroscopy [12] among others have been reported but they have shortcomings which include high cost, need for trained personnel and time consuming. Sensor systems have also been developed but they encounter problems such as limited sensitivity and the above mentioned. Some methods such as electrochemical methods were developed to address the above shortcomings but they are only applicable for a narrow range of concentration [9], [13], [14].

1.3. Nanomaterials

Natural or man-made particles with a diameter of 100 nm or less are referred to as nanomaterials whereas the particulates with diameter ranging from 1- 100nm are nanoparticles [15]. Nanomaterials can be classified as natural and synthetic based on their composition and shapes for example nanoparticles, nanowires, and nanotubes among others. Synthetic nanomaterials are normally associated with an enhancement in their properties which include surface area and chemical activity among others due to their altered surfaces. Their improved properties also include their catalytic properties which are useful in water purification through detection and removal of pollutants in water. Nanomaterials can be categorized into carbon- based NMs made of carbon quantum dots, carbon nanotubes, graphene oxide and fullerenes [16], [17]; metal-based NMs which include gold, silver, copper, titanium and zinc oxide and platinum among others [18], [19], [20]; dendrimers which are polymers of nanosized branched units; soft nanoparticles self- assemble which are nanoparticles formed by the self- assembly of individual molecules with varying physicochemical properties [21] and lastly nanocomposites which are nanoparticles made from a combination of different nanoparticles [22], [23].

Due to their small size, most of the characteristics possessed by the nanoparticles are not common in bulk materials [24]. Their size and optical properties influence their color and hence they have different colors. Just as their variation in color, they also have different morphologies which include nanofibers, nanosheets, solid, hollow or porous nanospheres among others [25]. The different sizes, morphologies and phases determines most of their properties and applications [21]. They are applicable in pharmaceuticals, chemical and biological sensing, environmental and even in cosmetic studies due to their properties which include size, shape,

morphology, porosity, surface area and chemical activity among others [26]. Their applications have led to a worldwide increase in nanotechnology investments. These investments have led to development of technologies capable of detecting pollutants in water, soil and air for quality improvement [27]. A rise in the investments in nanotechnology has also led to an increase in the interest on nanozymes development. Scientists are now working towards replacing natural enzymes due to their shortcomings with nanozymes.

1.4. Nanozymes

Nanozymes are nanomaterials capable of mimicking natural enzymes since they possess enzyme- like characteristics because they have properties of both enzymes and surface catalysts. They have advantages over natural enzymes which include stability, affordability, easy to store and recover, enhanced catalytic activity, accommodative of the environmental conditions, applicability in a wide range of temperature and pH among others, which qualifies them to be used for pollutant detection and remediation [25], [28]. The enzyme- mimicking ability of the nanomaterials include the following categories:

1.4.1. Peroxidase- mimic activity

This is the first activity to be discovered and more frequently used because the substrates used are common in many organisms. The nanomaterials used include metals, carbon- based and nanocomposites [29]. Catalysis in the presence of the substrates depends on temperature, pH, and concentration of the substrate. Peroxidase activity just as the name indicates incorporates the use of hydrogen peroxide and the substrate to undergo oxidation, and sometimes biomolecules are needed to complete the reaction following the Michaelis- Menten mechanism or the ping pong mechanism [30]. This catalytic activity is achieved by transfer of electrons or generation of reactive oxygen species. Electrons are transferred by the process of adsorbing the substrates onto the surface of the nanozymes thereby donating electrons to the surface which contains active sites permitting the redox reaction between the substrates and H_2O_2 leading to the reduction of H_2O_2 and oxidation of the substrate. In case of the ROS, the reaction between nanozymes and H_2O_2 produces the oxygen species which oxidize the substrates [25]. ROS includes groups like $\cdot OH$, $O_2^{\cdot}$, $HO_2^{\cdot}$ [31]. Examples of the assays for peroxidase activity include the positively charged gold nanoparticles which were discovered to possess intrinsic peroxidase activity and hence applied that property to detect H_2O_2 and glucose [32]. Chen *et. al.* [33] also proved that

cupric oxide nanoparticles have intrinsic peroxidase- like activity comparable to the horseradish peroxidase. Garg and Bisht [34] synthesized carbon nanodots possessing peroxidase-like activity and applied them in the detection of H_2O_2 and glucose.

1.4.1.1. Michaelis- Menten mechanism

This mechanism is normally employed to obtain the kinetic parameters of the catalytic activity [35], [36]. By use of the Michaelis- Menten equation, parameters such as K_m (Michaelis- Menten constant) and the V_{max} (maximal reaction rate) are obtained.

$$Vo = \frac{Vmax\ [S]}{(Km + [S])}$$

Where V_o is the initial velocity of the reaction and [S] is the substrate concentration. The K_m value determines the affinity of the catalyst to the substrate and it is equal to the concentration of the substrate at half of V_{max}. These parameters can also be calculated using the double- reciprocal of the Michaelis- Menten curve known as the Lineweaver- Burk plot. The absorbances can therefore be converted to concentration by employing the Beer lambert law $(A = \varepsilon bC)$ with ε as the molar absorptivity of the substrate and b as the path length [37].

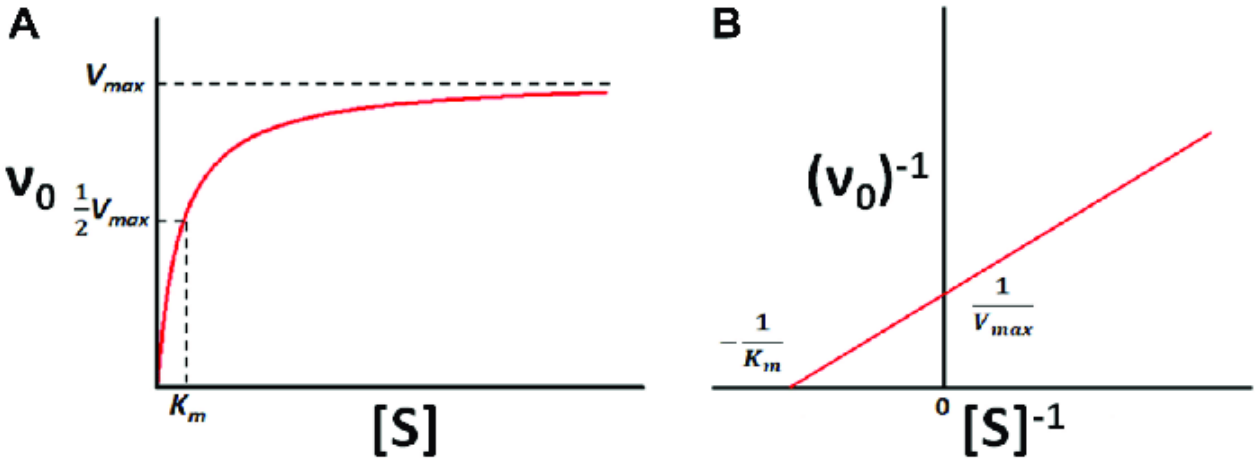


Fig 1.1. (a) Michaelis- Menten curve **(b)** Lineweaver- Burk plot [38]

1.4.1.2. Ping pong mechanism

This is a non- sequential mechanism which involves more than one substrate and is capable of releasing the product before both the substrates bind to the enzyme. It earned the name the ping pong mechanism because the enzyme keeps bouncing back and forth from its intermediate state back to the standard state. This mechanism also includes formation and release of one product first before the second substrate binds and the enzyme changing to the intermediate state when this occurs. The mechanism follows the reaction [39]:

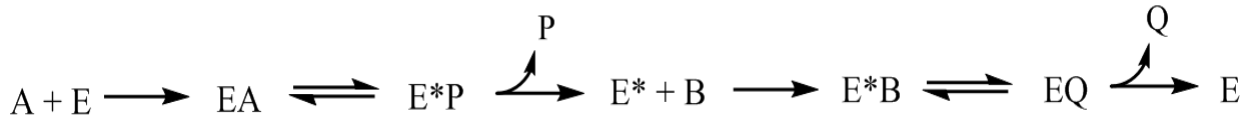


Fig 1.2. Ping pong reaction mechanism

A= substrate one, B= substrate two, E= enzyme, E*= enzyme intermediate, P= product one and Q= product two.

For this mechanism, the Lineweaver- Burk plot gives a series of parallel lines.

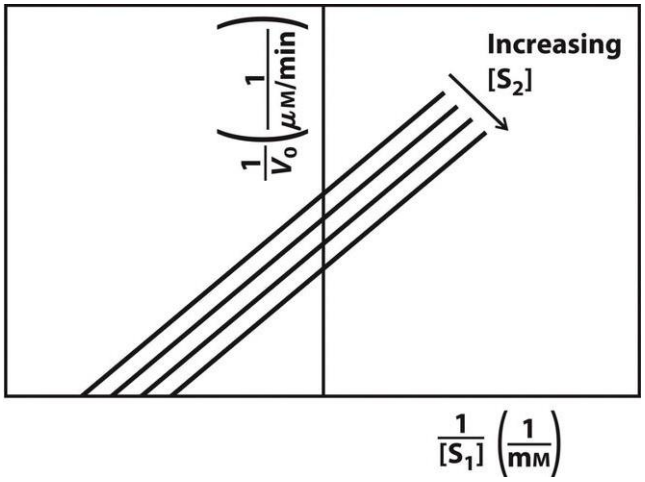


Fig 1.3. Lineweaver- Burk plot

1.4.2. Oxidase- mimic activity

Oxidase activity involves catalysis of the transfer of electrons from the substrate to the oxidized product or analyte under optimized conditions followed by production of H_2O or H_2O_2. Substrates normally used involve polyamines such as 2, 2'-azino-bis (3-ethylbenzothiazole-6-sulfonic acid (ABTS), o- phenylenediamine (OPD) and TMB because their oxidation states can give a visible color change and sensitive UV/ Vis absorption signal [40]. Oxidases aids catalysis by use of oxygen, which is an environmentally friendly oxidant, hence avoiding pollution. This activity is not commonly studied because most reviews focus on the peroxidase activity or superoxide dismutase hence it is significant that more attention be focused on this activity. Some of the nanomaterials that were developed based on this activity include the Nanoceria that was found to show oxidase- like activity in acidic solutions since it was able to oxidize organic substrates in the absence of H_2O_2 [41]. Guo *et al.* [42] also proved that Se NPs possessed intrinsic oxidase- like activity and catalyzed oxidation of TMB in the presence of dissolved

oxygen. Cheng *et al.* [43] developed a colorimetric detection method based on the oxidase- like activity of Pt NPs for detection of ascorbic acid.

1.4.3. Catalase activity

The catalase- mimic activity involves the catalysis of the redox reactions or adsorption for production of water and oxygen from H_2O_2 following the Michaelis- Menten mechanism. The activity is dependent on temperature, pH, nanoparticles morphology and structure and concentration of substrate. It is more efficient in alkaline or neutral systems. Its application includes the Nanoceria that was found to exhibit the catalase activity at the right concentrations of H_2O_2 following a redox reaction [44]. Singh and Singh [45] reported that a change in the phosphate buffer anions, pH or composition of cell culture media did not result in any effect in the catalase- mimic activity of CeNPs (4+).

1.4.4. Superoxide dismutase activity

This activity involves the dismutation of the toxic superoxide anions ($HOO^{\cdot}$ and $O_2^{\cdot -}$) into H_2O_2 and O_2 following the ping pong mechanism. The nanozymes aids the transfer of electrons in the system and the adsorption process. The activity is dependent on pH, nanozymes structures or surface ions. The superoxide- dismutase mimic activity was applied by Ali *et al.* [46] when they reported the potential of C_3 tris malonyl- C_{60} derivative (a fullerene compound) as a superoxide dismutase (SOD) mimetic.

1.4.5. Hydrolase

It is mostly applicable in biological systems by catalyzing the breaking down of chemical bonds by water.

The enzyme- mimic activity of nanozymes has been explored to develop colorimetric methods for detection of Cr^{6+} [42–46]. These methods can counter the shortcomings of the previously mentioned techniques and those of natural enzymes. They mainly base on the peroxidase activity hence making it the most common activity [47–52] while other activities such as the oxidase activity [36–38], [53], [54] have a few reviews hence the interest in this activity for this assay to try and give a rise to the assays based on this activity. The methods are easy to understand, cheap, have low detection limits and are highly selective and sensitive.

1.5. Statement of the problem

Because of the toxicity of Cr^{6+}, it was reported to cause gene mutations, DNA damages and chromosomal abnormalities and that leads to diseases such as lung cancer as well as infections to the kidneys and liver [58], [60]. It is due to this toxicity that there is a limit to the quantity of Cr^{6+} allowed in wastewater in accord to the World Health Organization (WHO) which is 0.005ppm. Some industries try to treat their wastewater for Cr^{6+} but the methods leave behind some concentration of Cr^{6+} which is still toxic to the environment. Therefore, the development of a simple, environmentally friendly, and cheap method that can detect Cr^{6+} within a short period of time is vital.

This study aims to come up with sensitive and selective methods for detecting Cr^{6+}.

1.6. Aims and Objectives

The main purpose of this assay was to develop a method for detection of Cr^{6+} based on enzyme-mimic property of copper-based nanomaterials. To fulfill the aim, the objectives to be followed included:

- To prepare copper-based nanomaterials with enzyme-mimic activities.
- To investigate the enzyme- mimic activity of copper-based nanomaterials.
- To determine Cr^{6+} based on enzyme-mimic activity of copper-based nanomaterials.

1.7. Significance of study

Due to an increase in industries as countries develop has resulted in increased pollution and at some point, safe drinking water will emerge to be scarce even though it is an important resource. As a result of pollution, humans are at a risk of ill health due to consumption of water containing toxins that are harmful to their bodies. Therefore, development of simple methods for detection of toxins in the natural waters and waste waters from industries will help address the problem of health defects due to consumption of polluted water. When employed together with methods that can remove the toxins, they will lead to natural waters being free from toxins hence safe water available for consumption.

1.8. Thesis Layout

This thesis will be made up of 5 chapters.

Chapter 1 gives a detailed introduction to heavy metals, nanomaterials and nanozymes and their examples. The significance, motivation, aims and objectives of the study will also be discussed.

The second chapter offers literature review on water pollution, methods for detection of chromium and copper- based nanoparticles.

Chapter 3 discusses the development of a copper- based nanocomposites sensor for the detection of chromium (VI) based on its oxidase- mimic property. The nanocomposites are characterized and optimized for sensitive and selective determination of the analyte and applied for real sample analysis.

Chapter 4 discusses on the development of a copper oxide sensor for detection of chromium (VI) based on the nanoparticles' oxidase- mimic property. These nanoparticles are characterized and under the best optimized conditions used for selective and sensitive determination of the analyte and application to real sample analysis.

Chapter 5 gives a conclusion of the results obtained and discussed and the recommendations.

CHAPTER 2: Literature review

2.1. Water pollution

Despite the fact that water is fundamental to sustain life on earth, its availability as safe drinking water is very scarce and hence a major challenge for the 21st century. Out of the 71% of the water making up the earth, only 1% of it is drinkable water [61]. This is due to the degradation in the water quality commonly referred to as water pollution. Water pollution refers to the presence of pollutants such as germs, toxic substances and also those substance that need too much oxygen to decompose, are radioactive and some are easily soluble in water bodies. These pollutants are in excess in such a way that they make the water unsafe for uses such as drinking, cooking, and bathing and so on [62], [63]. It occurs in places containing water such as rivers, oceans, valleys etc. The pollution is a result of those substance (s) requiring too much oxygen than the water source can offer to decompose and also being soluble in the water and hence keeps accumulating in the water source without being broken down [64]. The presence of pollutants in the water source can be referred to as contamination which refers to an increase in concentration (usually in ppm/ ppb) of a substance to a level that the water source and organisms cannot hold [65]. These substance (s) commonly known as pollutants includes heavy metals among others.

Water pollution is due to the existence of contaminants in water from waste and that waste can be categorized as municipal waste or industrial waste. Municipal waste is one that results from domestic or commercial activities while industrial waste is one from industrial and agricultural activities. The agricultural sector contributes to wastewater due to the use of chemicals and microorganisms for diseases and pests' control and on the other hand industries deal with metals, chemicals and mines procedures that generate waste. The agricultural waste is mostly rich in organic compounds while the industrial waste is rich in heavy metals, chlorinated by- products, organic and inorganic compounds [66]. These pollutants do not just end in the water sources because they find their way to mammalian cells. Taking heavy metals as an example, humans consume them either directly from the water source or from animals and plants. Plants get the toxins from the polluted soil as water pollution normally leads to soil pollution and the animals consume the plants and vegetation from the contaminated soil [67]. The heavy metals also end

up in human beings' bodies from eating sea food [68] that have been ingesting the pollutants as they swallow the water in the contaminated water systems.

Population growth leads to a spike in contamination of water and at the same time increasing its demand. Climate change also affects the water demand by leading to uneven distribution of fresh water since it influences when, where and how much precipitation falls, and also results in uneven rainfall that can lead to droughts. This water scarcity problem therefore forces people in some regions to resort to use of storm water, contaminated fresh water, waste water and sea water for their everyday water needs. The use of these waters depend on the existing water treatment technologies and infrastructure but nowadays even those are not efficient in improving the quality of water for human use [69]. Around 1.2 billion people do not have access to clean fresh water, 2.6 billion have very little access to it and millions perish yearly as a result of consumption of contaminated water [70].

2.2. Emerging contaminants

Water pollution can also be a result of the presence of emerging contaminants in water bodies. Emerging contaminants (ECs) refers to those contaminants that do not have regulations set for monitoring them or for reporting their presence in water. Their rise is also due to increased industries, agricultural production and also urbanization. These ECs include personal care products, pesticides, pharmaceuticals, cosmetics, surfactants, nanomaterials, food additives, drugs, micro plastics, cleaning products and so on. They are released into the water bodies as hospital effluents, industrial wastewaters, agriculture run- off, landfill leaches, domestic discharges and mainly through the treatment of municipal waste water. Conventional methods have been developed for determination of priority contaminants but were not designed for detection of emerging contaminants [71]. These ECs can result in hormonal interferences, cancer, immune toxicity, thyroid, resistance of bacteria to antibiotics, genotoxicity and endocrine disruption. They are normally synthetic or natural occurring chemicals or microorganisms that are difficult to monitor in the environment but has the capability to have adverse human and ecological effects. There is lack of advanced and efficient methods for determination of these contaminants due to their complexity and presence in low concentrations in water bodies [72].

Treatment methods have been developed for the determination of the ECs and they include oxidation, physico- chemical and biological methods but they have shortcomings such as

secondary pollution, high costs and need for skilled manpower due to complexity [73]. Adsorption, nanofiltration (NF), reverse osmosis (RO), electrochemical oxidation (EO) and advanced oxidation processes (AOPs) have also been found to be effective for the removal of these pollutants but some still suffer from the above- mentioned drawbacks [74] with EO and AOP encountering complications with mass transfer. Efficiency of the methods is proportional to the organic concentration. As a way to make the EO and AOPs more efficient, an ultrasound generator can be introduced in the system to encounter the problem with the mass transfer and electrohydraulic cavitation and also promote production of hydroxyl radicals by water decomposition. EO can also be coupled with ultraviolet light (photo- EO) to promote the generation and/ or activation of oxidizing agents [75].

2.3. Water status in Botswana

Botswana is a semi- arid country and that makes it vulnerable to drought and high temperatures [76]. The rainfall is low and there is high evaporation therefore Botswana experiences hydro-climatological water scarcity [77]. About 77% of the country is occupied by the Kalahari Desert which limits its supplies of fresh water [78]. The country also has low rates of groundwater supply even though that is the main source of domestic, agricultural and industrial water [79]. There are not many reports on the study of heavy metals in water in Botswana but those done prove that waste waters from nickel- chrome electroplating plants and tanning factories contain nickel and chromium which are harmful to human health [80]. The waste water from the Glen Valley treatment plant has been found to be re- used for irrigation after treatment but crops have been found to contain traces of nickel and chromium which can have detrimental effects to health [81]. Methods such as flame atomic absorption spectroscopy (FAAS), graphite furnace atomic absorption spectroscopy (GFAAS) and differential pulse adsorptive cathodic stripping voltammetry (DPAdCSV) have been employed for the determination of chromium and other metals [80].

2.4. Methods for detection of heavy metals in water

Methods including atomic absorption spectroscopy (AAS), anodic stripping voltammetry (ASV), instrumental neutron activation analysis (INAA), inductively coupled plasma mass spectrometry (ICPMS) and x-ray florescence (XRF) were used for detection of heavy metals in water [82] but their use encountered shortcomings such as high cost, short range of analysis, complexity and

time consuming [83]. AAS can only determine one element at a time and for a long time and it is also destructive. ASV is only applicable to metals that can form an amalgam and it is also prone to interferences from the matrix of the sample. ICPMS is not selective of the chemical forms or charge number of an element and very expensive. XRF is only applicable to thin films and surface layers. INAA requires a neutron source in order to become sensitive and that source is normally a nuclear reactor which needs a license to access it which makes it not readily available when needed for use [83]. These shortcomings led to an interest in the development of nanomaterials based methods for monitoring and detection of pollutants in water even in trace amounts [84]. Nanomaterials- based nano- sensors have therefore been synthesized from green or chemical methods for heavy metals detection in water. These methods have proved to have several advantages and thus raising interest in them. Some of their advantages include low limit of detection and quantification and also the ability to be applied on- site [85]. Ullah *et al.,* [86] and Waheed *et al.,* [87] outlined that nanomaterials- based nano- sensors have advantages over conventional methods including high sensitivity and selectivity and better performance of devices.

2.5. Detection of chromium

Among the pollutants found in water there are heavy metals as mentioned above and among those is chromium which is the pollutant of interest in this assay. Various analytical methods has been used for analyzing chromium including high performance liquid chromatography (HPLC), atomic absorption spectroscopy (AAS), inductively coupled plasma- mass spectroscopy (ICPMS), capillary chromatography, spectroflourimetry, spectrophotometry and chemiluminescence among others [88]. For speciation and trace element analysis, two or more techniques can be combined [89], [90], [91]. However, they have shortcomings which include time- consumption, experienced personnel for operation, sample pre-treatment before analysis and high expenses. Therefore, since chromium (VI) demands the need for monitoring techniques it is of importance to develop rapid, portable, low cost, simple and on- site methods that can give immediate results [88].

Conventional methods such as graphite furnace- AAS (GF- AAS) [92], and liquid chromatography- ICPMS (LC- ICPMS) [93], [94] have been also been applied for detection of chromium (VI), but they also have shortcomings which include sample preparation which is time

consuming and requirement for skilled personnel [52] and the difficulty in differentiating the oxidation states of chromium among the aforementioned has led to a rise in the interest of colorimetric methods [95]. Surface enhanced Raman spectroscopy (SERS) has been applied for the detection of chromium with high sensitivity and rapid detection [96], [97] but faces the challenge of poor reproducibility of measurements [98]. Localized surface plasmon resonance (LSPR) was discovered to have the ability to detect chromium (VI) with high sensitivity and simplicity but it is only sensitive for low concentrations [99], [100]. The shortcomings of these methods allowed for development of colorimetric methods involving nanozymes and the enzyme- mimic activity[55], [58]. The popular nanozymes include precursors such as silver and gold which are noble metals and very scarce leading to a gap that allows for use of precursors found in abundance. That gap allowed for interest in copper as a precursor since it is available in abundance on the earth's surface [101].

2.6. Copper- based nanoparticles

Copper is an easily accessible, environmental friendly and cheap metal since it is found in large amounts on earth and that has made it a metal of interest since it can be used in place of noble metals such as silver and gold that are scarce [101]. Copper- based nanoparticles have since become of interest due to the abundance and availability of copper and due to its attractive chemical and physical properties. Some properties like its high boiling point allow it to undergo chemical reactions at high pressure and temperature and the wide range of oxidation states allows it to undergo different reactions [102]. Its properties including the high activity and surface area have gained copper-based nanoparticles popularity in fields such as catalysis, medicine, pharmaceuticals, electronics, water purification and catalytic organic transformations among others [103].

2.7. Synthesis of copper- based nanoparticles

Synthesis of these nanoparticles is by hydrolysis, reduction, oxidation, and condensation chemical reactions. Method selection is highly dependent on the type of nanoparticles to be obtained. In case of copper nanoparticles the reduction process is used, hydrolysis followed by dehydration are normally used for copper oxide nanoparticles and oxidation for copper- based nanoparticles [102]. For better application of the nanoparticles, synthesis methods such as wet chemical and solution- phase can be used to allow for control of the size, shape, morphology,

crystallinity, and other properties of the nanoparticles. This control is obtained through the choice of solvents, capping agents, temperature and time of reaction [104]. This assay employs the use of the solvothermal method which is a solution- phase method for preparation of copper-based nanoparticles possessing enzyme- mimic activity.

2.7.1. Solvothermal method

Synthesis following this method entails heating of solvents to a temperature higher than their boiling points under pressure in a Teflon- lined stainless- steel autoclave. The high pressure and temperature increase the solubility and reactivity of the reactants. Its ability to be applicable under high pressures makes it suitable for synthesis of high- quality nanocrystals such as metal oxides, nitrides, and semi- conductors. This method is capable of producing nanocrystals that have a narrower size distribution and high crystallinity than other methods [105]. The means to manage the morphology of the particles using this method makes it reliable and reproducible. Control of the morphology is reliant on factors such as temperature, solvent effects, reaction time, and ligand effects among others [104].

In summary, reports have been made on the presence of chromium (VI) in aquatic systems and treated waste water from industrial and domestic use. Different concentrations have been recorded all over the world in water bodies for example, 0.580 mg/ L was once reported at Hinkley, California [106], 50 mg/ L in Leon Valley [107], Mexico and 16.3 mg/ L in Kanpur, India [108] just to name a few as a result of industrial runoff or poor waste disposal. The health effects related to consumption of chromium (VI) are detrimental hence it is of high necessity to monitor it in the environment and have effective methods in place for its rapid detection.

CHAPTER 3: Chromium (VI) detection based on the enhanced oxidase- like activity of the recoverable CuS/ Fe_3O_4 composite

3.1 Introduction

There are a number of oxidation states for chromium and they possess varying properties. Among them there is chromium (III) and (VI). The solubility of Chromium (III) allows it to take part in cellular reactions and that makes it safe even when it finds way into mammalian cells [109]. Chromium (VI) is mainly released to water bodies by industrial processes including leather tanning, metal plating, textile dyeing among others and that makes it a toxin to mammalian cells [110]. Its detrimental effects on humans and animals led to organizations such as the World Health Organization (WHO), [3] setting its maximum concentration in water as 0.005 ppm hence the urgency to come up with sensitive assays for its detection.

Techniques such as chromatography [4], mass spectrometry [5], and electrochemical [6] were developed earlier for determination of chromium (VI). They fell short regarding the detection of chromium (VI) due to draw backs like complexity which requires trained operators, expensive and time- consuming processes. Alternatives that resulted as an address to those drawbacks included colorimetric methods since they could counter them as they proved to be simple, cheap and fast in analysis. Localized surface plasmon resonance (LSPR) by gold and silver

nanoparticles is one of the methods developed for detection of chromium (VI) [7]. The enhancement of the signal demands controlled particle- analyte distance, surface charges and particles surfaces [8]. Colorimetric methods based on catalysis have been recommended to counter these problems [8]. The report of the magnetic nanoparticles (Fe_3O_4) possessing enzyme mimic activity [9] led to the use of nanozymes as signal amplifiers for determination of analytes using colorimetric methods common [10].

Nowadays, there has been various reports for detection of Cr (VI) basing on the enzyme- mimic activity of nanomaterials. For example, Qi *et al.,* recently explored the peroxidase activity of citrate- capped gold nanoparticles for determination of Cr (VI) [11]. Zhang *et al.,* [12] determined Cr (VI) basing on the peroxidase activity of the ternary nanohybrid material that contains gold nanoparticles, hyper branched polyethylenimine (PEI) and reduced graphene oxide. Ghayyem *et al.* (2021) [13] discovered that poly (N-phenylglycine) nanoparticles possessed peroxidase- mimic activity and used that property to determine chromium (VI). There are also reports that explore the detection of Cr (VI) based on the oxidoreductase- or oxidase-like activity of nanomaterials [14-16]. These assays do not use H_2O_2 which is unstable hence complicating the repeatability of measurements and also harms the environment [17, 18] and that broadens the applicability of nanoparticles in the field of analysis. Reports on application of oxidoreductase- and oxidase- like activity are still few compared to the peroxidase- like activity and that leaves room for discovery of more of those assays. A lot of these reports are synthesized by use of noble metals which are expensive thus their use for detection of Cr (VI) is discouraged [11, 15, 16]. The use of nanozymes synthesized from noble metals is also limited by issues such as control of the charge on the surface of the particles, plasmonic interferences and problems with the stability of the nanomaterials for a long time [11, 15] and all these issues need to be addressed.

The combination of different catalysts to form composites has become popular for affirming the catalytic activity due to the synergy effect of the individual components [9, 19-20]. The activity of the composites was found to be higher than that of the separate individual components [19, 21- 22]. Hence it is of importance to develop functional nanocomposites for the enhancement of the enzyme- mimic activity [111].

In this assay, a composite of CuS and Fe_3O_4 was prepared in order to enhance the enzyme-mimic activity. The magnetic property of Fe_3O_4, allows for easy separation of the particles from the mixture thus avoiding background interferences that can result from the suspended particles of CuS when used alone during UV/Visible spectroscopy analysis of oxidized oxTMB. CuS offers dispersibility and stability for the composite. The synergy effect of CuS and Fe_3O_4 enhanced the catalytic activity in the presence of oxygen as the green oxidizing agent rather than the unstable H_2O_2 molecule. The composite is cost- effective and stable compared to the noble metals based nanozymes detection system. Since it does not use mercury there is no secondary pollution formed like in the detection of chromium using Au@Hg [15]. The composite was used in deionized water to detect Cr (VI) with a broad linear range and high selectivity. The method was applied to tap water and proved its feasibility to real sample analysis.

3.2 Experimental

3.2.1 Chemicals

Reagents of analytical grade and Millipore deionized water were used to prepare aqueous solution without further purification. Potassium chloride and ferric chloride were bought from Associated Chemical Enterprise (ACE) (Johannesburg, RSA). Potassium dichromate and nickel sulphate were from Minema (Roodepoort, RSA). Chromic chloride, potassium permanganate, mercuric sulphate, zinc nitrate hexahydrate, sodium nitrite, were purchased from MERCK (Gauteng, RSA). Calcium chloride dihydrate, ferrous sulphate hydrate, ethylene glycol, silver nitrate, sodium sulphite, urea, tri-sodium citrate, and thiourea were purchased from Rochelle Chemicals (Johannesburg, RSA). Dimethyl sulfoxide and acetic acid were from Sigma Aldrich (France). Copper (II) nitrate trihydrate was purchased from Alpha Chemika (Mumbai, India). Lead (II) nitrate, mercuric nitrate, sodium acetate and magnesium acetate tetrahydrate were obtained from Sigma Aldrich (Germany). TMB was purchased from Sigma Aldrich (Switzerland). Copper (II) acetate monohydrate was from Sigma Aldrich (St Louis, USA). Cobalt (II) chloride was purchased from UNIVAR (Muldersdrift, RSA). Barium chloride dihydrate was bought from Sigma Aldrich (Japan).

3.2.2 Instrumentation

Field emission scanning electron microscope (Tescan MIRA 3 GMH, Czech Republic) operating with an electron energy of 5 keV and a probe current of 60 pA was used to obtain SEM images

of particles. The EDX spectra was obtained from a Zeiss Evo MA 25 SEM equipped with an EDAX Appollo X EDS (Jena, Germany) detector system operating at an electron energy of 10 keV and a probe current of 1 nA. X-ray diffraction (XRD) patterns of the particles were obtained on a D2 phaser XRD-300W powder diffractometer (Bruker, AXS GmbH, Karlsruhe, Germany) for a 2θ range of 10° to 90° at a scan rate of 0.05°/s using Cu Kα radiation at 40 kV and 100 mA. Thermo-Fischer UV/Visible spectrophotometer was used to collect UV/Visible absorption spectra.

3.2.3 Preparation of Copper Sulphide

A hydrothermal method obtained from literature was employed to synthesize the copper sulphide (CuS) nanoparticles with few modifications [23]. To a beaker containing 30 mL of deionized water and 40 mL ethylene glycol, about 1.9965 g of copper acetate and 0.9896 g thiourea were dissolved. The solution was moved to an autoclave then heated in the oven for 4 hrs at 160^{o}C. The green precipitate in the autoclave was allowed to cool overnight. After cooling it was washed with ethanol and deionized water several times before being dried in the oven for 4 hrs at 70 ^{o}C. The supernatant was discarded with the aid of centrifuging for 15 min at 12000rpm.

3.2.4 Synthesis of CuS/Fe_3O_4 composites

To 40 mL of deionized water; 0.5 g of ferric chloride, 1.2 g of tri-sodium citrate and 0.3 g of urea were dissolved and then 0.075 g of the CuS nanoparticles was added and allowed to stir magnetically for 30 min (adopted from literature with modifications) [112]. It was then moved to an autoclave and heated for 4 hrs at 200°C. The precipitate was allowed to cool overnight and later washed with deionized water. Magnetic decantation was applied when washing the nanocomposites.

3.2.5 Preparation of solutions

A 10 mM stock solution of TMB was prepared using the appropriate mass in a 25 mL volumetric flask and from it the required concentrations were prepared in 2 mL Eppendorf tubes using dimethyl sulfoxide (DMSO) as the solvent. The tubes were wrapped with aluminum foil and stored in a dark place. Acetate buffer (pH 4.0) was prepared using anhydrous sodium acetate (0.99g) and acetic acid (2.218 mL) and diluted to the mark with deionized water in a 250 mL volumetric flask. Buffers used to investigate the effect of pH were prepared from stock solutions of dibasic sodium phosphate and citric acid prepared in 250 mL volumetric flasks using

deionized water as the solvent. The interference molecules used for selectivity study were prepared in 50 mL volumetric flasks using the appropriate masses (400 µM). Potassium dichromate stock solution (2 mM) was prepared in a 100 mL vol. flask using deionized water as the solvent.

3.2.6 Synergy effect

To investigate if the interaction between two nanoparticles will enhance the absorbance, two individual nanoparticles and their composite were studied. The enhanced activity expected due to the synergy effect of the two individuals in the composite were studied by placing 2.0 mg of Fe_3O_4 or CuS or CuS/ Fe_3O_4 nanoparticles, 1.6 mL of acetate buffer (pH 4. 0), 200 µL of 3 mM TMB and 200 µL of 100 µM of Cr (VI) or deionized (DI) water for the control then incubating for 5 min on a shaker. Within the 5 min the mixture was transferred to a cuvette with a magnet placed under the cuvette to hold the particles to the bottom of the cuvette to avoid interference with the light and for the CuS which were not magnet, the mixture was centrifuged for 30 sec and the supernatant transferred to the cuvette. At exactly 5 min the absorbance of the mixture was measured using a UV/ Visible spectrophotometer from a range of 300 to 800 nm.

3.2.7 Enzyme-mimic activity of the CuS/Fe_3O_4 nanocomposites

The catalytic activity of the particles was investigated based on the oxidation of TMB as the substrate. The change of color of TMB from colorless to the blue- colored oxTMB upon addition of Cr (VI) allowed for the assessment of the enzyme- mimic activity of the nanocomposite. Reaction mixtures including TMB only; TMB, and chromium (VI); TMB and CuS/Fe_3O_4; TMB, chromium (VI) and CuS/Fe_3O_4 (all in acetate buffer of pH 4.0) were incubated before being transferred to a cuvette. The CuS/Fe_3O_4 were allowed to settle at the bottom of the cuvette to avoid interference with the aid of a magnet. The whole process was done under 5 min and at 5 min (using a stopwatch) the UV/ Visible spectrophotometer was used to measure their absorbance from a range of 300- 800nm.

3.2.8 Optimization of parameters

A sensitive method which is the aim of this assay requires the use of parameters that give the maximum absorbance and in order to obtain those a method needs to be optimized. In this assay the pH of the buffer, catalyst load and concentration of TMB were optimized and the optimum values for the parameters used for further analysis.

3.2.9 Optimization for mass

To a 2 mL Eppendorf tube containing different mass of catalyst (1.0 to 3.0mg), 1.6 mL of acetate buffer (pH 4.0), 200 µL of 3 mM TMB and 200 µL of 100 µM of Cr (VI) or DI water for the control were added and incubated for 5 min on a shaker. Within the 5 min the mixture was transferred to a cuvette and at 5 min its absorbance was measured. The measurement for each mass was repeated three times and the average used for comparison with the others in order to determine the optimum mass.

3.2.10 Optimization for pH

Buffers of pH ranging from 2.6 to 7.0 were used to carry out this optimization study in order to determine the optimum pH. To a 2 mL Eppendorf tube containing the optimized mass of catalyst (2.5 mg), 1.6 mL of varying buffers, 200 µL of 10 mM and 200 µL of 400 µM Cr (VI) were added and the mixture incubated for 5 min before being transferred to a cuvette to measure absorbance. Buffers of different pH were used in each measurement and each pH was run three times.

3.2.11 Optimization for concentration of TMB

To a 2 mL Eppendorf tube 2.5 mg of CuS/ Fe_3O_4, 1.6 mL acetate buffer (pH 4.0), 200 µL of varied concentrations of TMB (1 to 10 mM) and 200 µL of 100 µM Cr (VI) or DI water as control were added and the mixture incubated for 5 min. After the 5 min, the mixture was transferred to a cuvette to measure absorbance. Each concentration of TMB was run three times.

3.2.12 Colorimetric detection of chromium (VI)

The impact of dissolved oxygen was investigated by purging the buffer solution to be used in the experiment with nitrogen and comparing the absorbance it gives with that of unpurged buffer. A mixture containing the CuS/ Fe_3O_4 nanoparticles (2.5 mg), a purged or unpurged 1.6 mL acetate buffer (pH 4.0), 200 µL of 6 mM TMB and 200 µL of 400 µM Cr (VI) was incubated for 5 min on a shaker and their absorbances measured using a UV/ Vis spectrophotometer. This was further investigated by the use of scavenger molecules, p- benzoquinone ($O_2^{\bullet-}$ scavenger) and t-butanol ($^{\bullet}OH$ scavenger) with DI as the control. Mixtures containing the CuS/ Fe_3O_4 (2.5 mg), 100 µL of DI water or p- benzoquinone (5 µM) or t- butanol (10 mM), 1.6 mL acetate buffer (pH 4.0), 200 µL of TMB (6 mM) and 100 µL of 400 µM chromium (VI) were incubated for 5 min and their absorbances measured and compared.

The detection of Cr (VI) was done by placing 2.5 mg of CuS/ Fe_3O_4 in a 2 mL Eppendorf tube

and adding 1.6 mL of acetate butter (pH 4.0), 200 µL of 6 mM TMB and 200 µL of 400 µM Cr (VI) or DI water as the control. The mixture was incubated for 5 min before measuring its absorbance using a UV/ Vis spectrophotometer following the absorption range from 300 to 800 nm.

3.2.13 Steady state kinetics assay

The steady state kinetics experiments were carried out to investigate the catalytic activity of the CuS/ Fe_3O_4 nanocomposites. Reaction mixtures made of optimized conditions and varying concentrations of Cr (VI) had their absorbances being measured at different time intervals for each concentrations. The absorbance (654 nm) against time graphs were plotted for each concentration of Cr (VI). By employing the Beer Lambert's law to the slopes from the graphs, the initial rates or velocities were obtained.

$$A = \varepsilon l C \qquad \text{Beer Lambert law}$$

A= absorbance,

ε= is the molar absorptivity,

l= path length and

C= concentration

$$\text{When rearranged: } C = \frac{A}{\varepsilon l}$$

The initial rates or velocities were then calculated as follows;

$$\text{Initial velocities} = \frac{\Delta C}{\Delta t} = \frac{\Delta A/\Delta t}{\varepsilon l} = \frac{slope}{\varepsilon l}$$

A plot of the initial velocities against the concentrations gave the Michaelis- Menten curve. Its double reciprocal which is the Lineweaver- Burk plot allows us to derive the kinetic parameters, V_{max} and K_m using the equation;

$$\frac{1}{V} = \frac{1}{Vmax} + \frac{Km}{Vmax \cdot [S]}$$

Where, $\frac{1}{V}$ is the y- axis and $\frac{1}{[S]}$ is the x- axis,

With $\frac{1}{Vmax}$ as the y- intercept and $\frac{Km}{Vmas}$ as the slope of the equation.

The V_{max} allows us to comment on the enzyme- mimic activity of the particles in the presence of Cr (VI) while the K_m value allowed us to comment on the binding affinity of the particles with regard to Cr (VI).

3.2.14 Sensitivity

This study was performed following the procedure for colorimetric detection of Cr (VI) and using the optimized conditions. The concentration of Cr (VI) was varied from the lowest (0.0 µM, which is basically DI water) to 1900 µM. Each concentration was run three times and the average absorbance used to plot the calibration curve which involved the concentrations that can make a linear plot (0.0 to 1500 µM) and with its aid parameters such as the limit of detection (LoD) and limit of quantification (LoQ) were calculated.

3.2.15 Selectivity

The study used the optimized conditions and followed the procedure for detection of Cr (VI). In this case 200 µL of 400 µM of interfering metal ions and anions were used in place of chromium (VI). Various cations such as Ag^{+}, Ba^{2+}, Ca^{2+} Co^{2+}, Cr^{3+}, Cr^{6+}, Cu^{2+}, Fe^{2+}, Fe^{3+}, Hg^{2+}, K^{+}, Mg^{2+}, Na^{+}, Ni^{2+}, Pb^{2+}, Zn^{2+}, and anions such as NO_3^{-}, NO^{2-}, SO_3^{2-}, SO_4^{2-}, MnO_4^{-}, and Cl^{-} were evaluated. Chromium (VI) was also included for comparison. Each interference was run three times and their average absorbances were compared using bar graphs. A binary mixture which involved 100 µL of 400 µM for both Cr (VI) and the interference was also studied to investigate the sensitivity of the method for Cr (VI) even in the presence of the interference. To investigate the high response in the presence of MnO_4^{-}, a reaction mixture containing acetate buffer (pH 4.0), 6 mM TMB and MnO_4^{-} without the CuS/ Fe_3O_4 was incubated for 5 min and its absorbance measured and compared to the one obtained in the presence of CuS/ Fe_3O_4.

3.2.16 Real sample analysis

A 2 mM stock solution of potassium dichromate was prepared using tap water as the solvent in a 100 mL volumetric flask. Working standards of different concentrations were prepared from the stock in 2 mL Eppendorf tubes filling to the appropriate volumes with tap water. The analysis was done following the same procedure as that of sensitivity with each concentration having three runs.

3.3 Results and Discussion

3.3.1 Characterization of CuS/Fe_3O_4

The composite CuS/Fe_3O_4 was synthesized by first preparing the CuS nanoparticles then incorporating them in the process of preparing the Fe_3O_4 nanoparticles following a hydrothermal method. The presence of the Fe_3O_4 nanoparticles provide the nanocomposite with magnetic

property. The prepared nanocomposites were then characterized using techniques like scanning electron microscopy (SEM), energy dispersive x-ray spectroscopy (EDX) and X- ray diffraction (XRD). SEM was applied to explore the surface morphologies of Fe_3O_4, CuS and CuS/Fe_3O_4. The SEM images of Fe_3O_4 show the development of uniform microspheres as displayed in **Fig. 3.1a**. The CuS nanoparticles have irregular shapes with a rocky appearance and rough surfaces (**Fig. 3.1b**). As for the composite, unidentifiable spherical images were observed (**Fig. 3.1c**). In addition the EDX data for Fe_3O_4 (black curve) and CuS (red curve), show the presence of the following elements; copper, oxygen, Sulphur and iron (**Fig. 3.1d**). The EDX spectrum for the composite displays all the elements found in the individuals' spectrums which indicates successful formation of the composites. Moreover, the elemental mapping images of O (blue), Cu (orange), S (purple), and Fe (yellow) (**Fig. 3.1 (d-h)**) shows that CuS/Fe_3O_4 was made of O, Cu, S and Fe elements which are uniformly distributed in the composite.

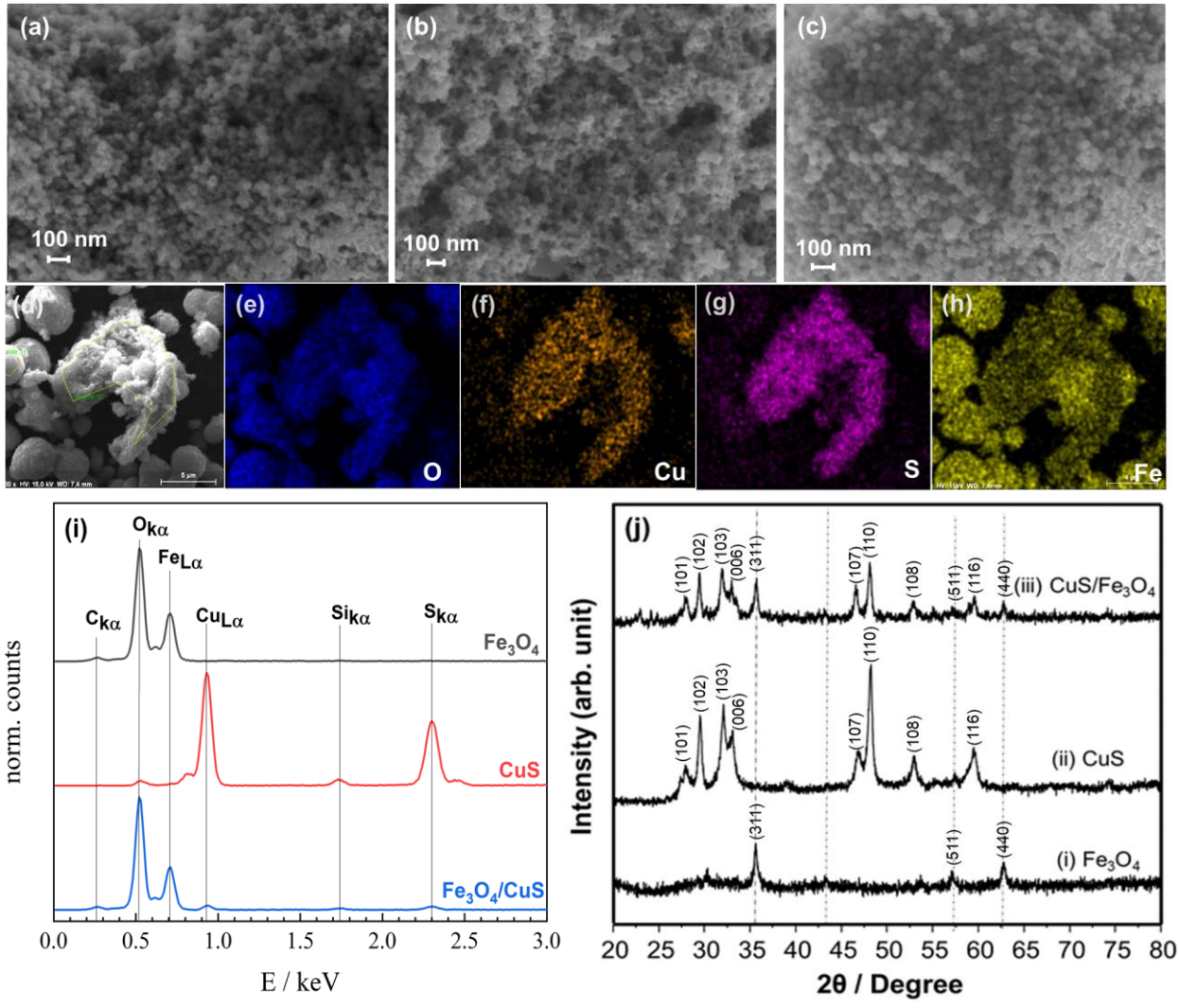


Fig. 3.1. SEM images of (a) Fe_3O_4 (b) CuS and (c) CuS/Fe_3O_4. (d-h) Elemental mapping for O, Cu, S, and Fe, (i) EDX spectra of Fe_3O_4, CuS, and CuS/Fe_3O_4. (j) Powder XRD patterns of Fe_3O_4, CuS, and CuS/Fe_3O_4.

XRD was also employed to analyze the crystallinity of the nanoparticles and the composite. The Fe_3O_4 nanoparticles possessing superparamagnetic property had diffraction peaks at 2θ angles of 35.74°, 57.04° and 62.60° that can be assigned to the indices (311), (511), and (440) lattice planes of the face-centered cubic phase of Fe_3O_4 [24, 25]. The CuS diffraction peaks were observed at 27.87°, 29.30°, 32.04°, 33.0°, 46.9°, 48.25°, 52.88°, and 59.36° which attribute to (101), (102), (103), (006), (107), (110), (108) and (116) planes of the hexagonal phase [113]. The discovery of the same peaks indexed for CuS and Fe_3O_4 on the XRD profile for CuS/Fe_3O_4 composites indicates that the synthesis of CuS/Fe_3O_4 composite was successful. By employing the Scherrer's formula, the average crystallite size of the composites was calculated as 14.6 ± 6.4 nm. The EDX, SEM and XRD data support successful preparation of the CuS/Fe_3O_4 composite.

3.3.2 Catalytic activity of CuS/Fe_3O_4

In the presence of TMB only in the buffer, the mixture remained colorless and hence recorded no notable absorbance Fig. 3.2a (**black curve**). With TMB and chromium (VI) in the acetate buffer, the mixture is too pale and there also recorded a very low absorbance even though it was better that of TMB only (green curve in **Fig. 3.3a**). The pale blue color change is a result of the ineffective electron transfer between TMB and chromium (VI). With TMB and CuS/Fe_3O_4 present in the mixture, it showed a noticeable color change and absorbance (red curve) which confirmed the catalytic activity of CuS/Fe_3O_4 in the presence of oxygen. A reaction mixture with TMB, chromium (VI) and CuS/Fe_3O_4 gave a high absorption peak which confirms that there was remarkable oxidation of TMB (blue curve) brought about by the efficient electron transfer between TMB and chromium (VI) via CuS/Fe_3O_4 connection.

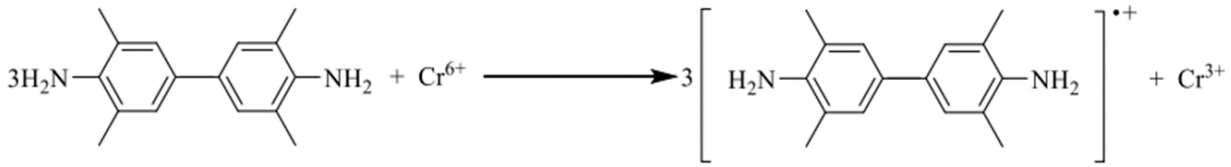


Fig 3.2. Reaction between TMB and Cr (VI) in the presence of the nanocomposites.

The citrate groups on the surface of CuS/Fe_3O_4 composite that are negatively charged are capable of attracting the positively charged TMB (cations in acidic pH) and initiate electron transfer [11]. The acidic pH favors formation of anionic chromium species such as $Cr_2O_7^{2-}$, $HCrO_4^-$ and positively charged species, $FeOH_2^+$ that allows for electrostatic adsorption of chromium (VI) on the surface of Fe_3O_4 [27]. This results in favorable conditions necessary for transfer of electrons between TMB and chromium (VI) leading to enhancement of the catalytic activity of CuS/Fe_3O_4 for oxidation of TMB with chromium (VI) present [11, 15]. The direct proportionality between concentration of chromium (VI) and absorption of oxTMB resulted in the development of this method for quantitative detection of chromium (VI).

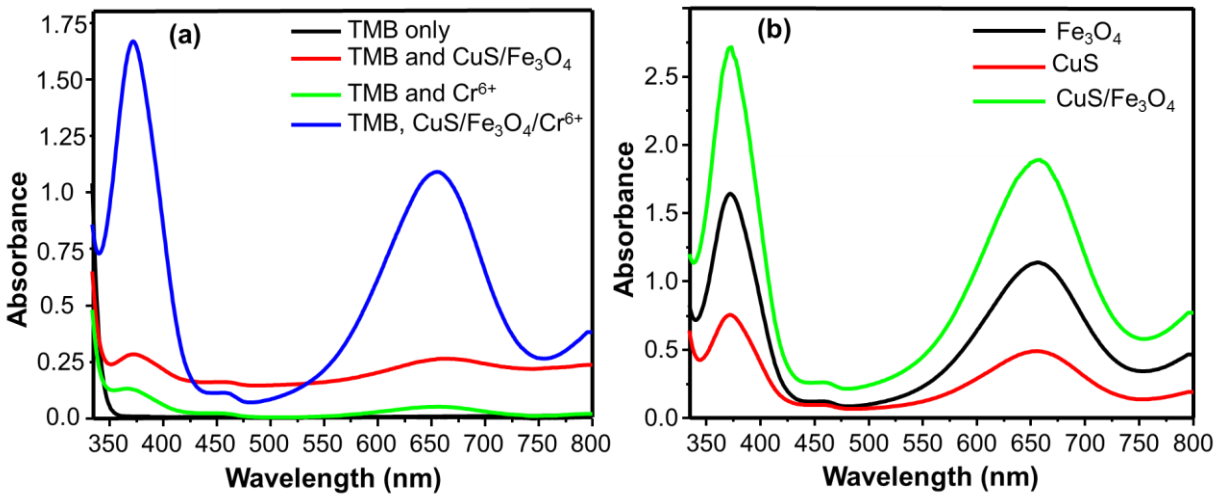


Fig. 3.3. (a) UV/visible absorption spectra for reaction systems in the presence of TMB only; TMB and CuS/Fe_3O_4; TMB and chromium (VI) and TMB, CuS/Fe_3O_4 and chromium (VI). (b) UV/visible absorption spectra of oxTMB using Fe_3O_4, CuS, and CuS/Fe_3O_4 with chromium (VI) present. Incubation time was 20 min.

The reaction of CuS, Fe_3O_4, and CuS/Fe_3O_4 to oxidation of TMB with chromium (VI) present was also investigated. **Fig. 3.3b** shows that even though CuS and Fe_3O_4 as individuals managed to enhance the oxidation of TMB, the highest and better enhancement was observed in the presence of CuS/Fe_3O_4. This proves the impact of the synergy energy between the two individual components making up the composites [21]. This observation therefore derives to the use of CuS/Fe_3O_4 instead of CuS and Fe_3O_4 separately since the composite allows for high sensitivity and improved analytical performance for detection of chromium (VI). The improved analytical

performance which includes factors such as wide linear range will be explored more in the succeeding section.

The importance of molecular oxygen on oxidation of TMB was investigated in order to show the mechanism of the oxidase-mimic activity of CuS/Fe_3O_4. One reaction system had dissolved oxygen being removed from the system by purging with nitrogen and the other included dissolved oxygen since there was no purging performed. **Fig. 3.4a** shows that in the presence of oxygen there is high catalytic activity of CuS/Fe_3O_4 as compared to the one that was purged as shown by the literature that was recently published [28]. In order to back up this observation, the main reactive species needed for the oxidation of TMB were explored by incorporating scavenging molecules in the reactions. Since the main reactive species expected to be present included the superoxide anion ($O_2^{\bullet -}$) and hydroxyl radical ($^{\bullet}OH$), *p*-benzoquinone and *t*-butanol were used as the scavenger molecules respectively.

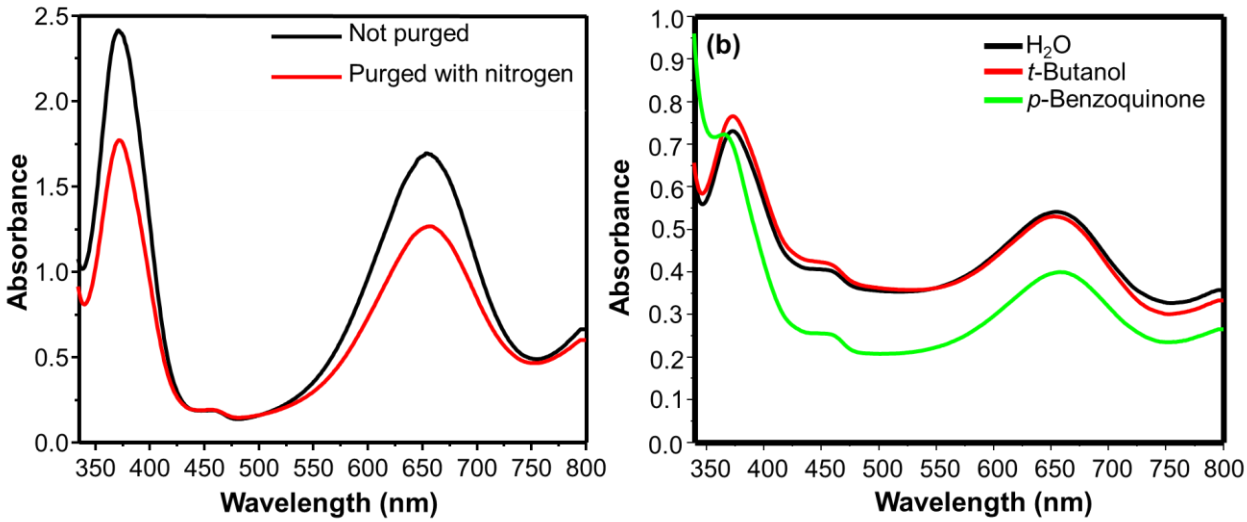


Fig. 3.4. (a) UV/visible spectra for TMB showing impact of oxygen on oxidation of TMB. (b) UV/visible absorption spectra for TMB solution in the presence of H_2O, *p*-benzoquinone and *t*-butanol.

A system that contains water (as control) and that containing *t*-butanol had absorbance peaks that were not that distinct from each other (black and red curves respectively). This tells us that *t*-butanol has no quenching role (towards $^{\bullet}OH$) which proposes that $^{\bullet}OH$ is not involved in the oxidation of TMB thus it is not produced during the reactions. The presence of *p*-benzoquinone

on the other hand shows an impact on the oxidation of TMB as we observe it being hindered **Fig. 3.4b** (green curve). This proves that $O_2^{\bullet -}$ is the main reactive species that is needed for the oxidation of TMB and since it is being quenched in the presence of p-benzoquinone there is a hindrance resulting in low absorbance's. This confirms that the superoxide anion is formed from the catalytic decomposition of molecular oxygen as indicated by Cai *et al.,* [29]. The Fe^{2+} found in magnetic nanoparticles donates an electron to O_2 to form $O_2^{\bullet -}$ hence its formation is favored by a magnetic nanoparticles suspension [30].

3.3.3 Optimization of the catalytic performance of CuS/Fe_3O_4 in sensing chromium (VI)

A number of parameters we optimized in order to maximize the performance of CuS/Fe_3O_4 nanocomposite in detecting chromium (VI) based on the oxidase-mimic activity of CuS/Fe_3O_4. The pH of the reaction mixture is one of the meaningful parameters in the oxidation of TMB as the amino groups of TMB are capable of undergoing transfer of protons. Oxidation of TMB which is due to the protonation of one of its amino groups normally happens at pH ranging from 4.0 to 5.0 [31]. Our data also agrees with literature as we witness absorption peaks which correspond to oxidation of TMB in all the acidic buffers tested [28, 32], so that in acidic conditions there will be conversion of molecular oxygen to $O_2^{\bullet -}$ for effective oxidation of TMB to oxTMB. **Fig. 3.5a** shows that the maximum peak is obtained at pH 4.0 and that shows the highest oxidase- like activity.

Among the important parameters to optimize is the amount of the catalyst [21]. An increase in absorbance was witnessed as the mass of the catalyst increased **Fig. 3.5b**. A significant difference between a system containing and one that does not contain chromium (VI) proves that the method is highly sensitive of chromium (VI) and 2.5 mg proved to be the optimum mass for this assay.

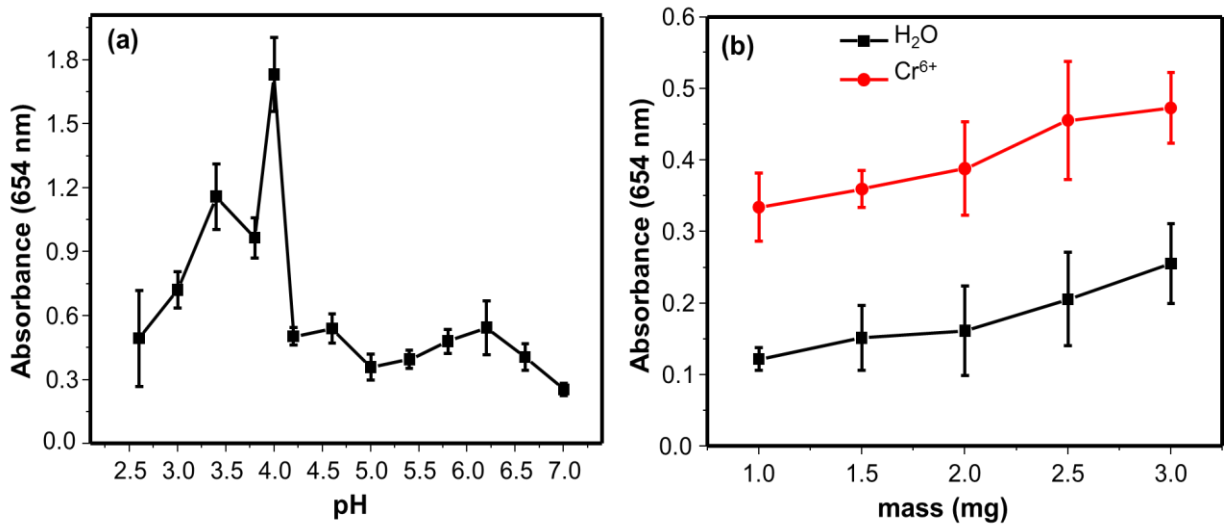


Fig. 3.5. (a) The impact of pH of the buffer on the oxidase-like activity of CuS/Fe_3O_4 in the presence of chromium (VI) (b) Impact of mass of CuS/ Fe_3O_4 on oxidation of TMB in the absence and presence of 100 µM chromium (VI).

A system that had the same volume of chromium (VI) replaced with H_2O showed no outstanding contrast in the absorption intensities and that proves the impact the presence of chromium (VI) has on the oxidase-like activity of CuS/Fe_3O_4. With chromium (VI) present in the reaction system, there was an increase in the absorbances from 1 to 6 mM (**Fig 3.6**) and thereafter there was no notable change in absorbance as the concentration of TMB increased and therefore 6 mM was used as the optimum. This scenario shows that before 6 mM the reaction is 1^{st} order and from 6 Mm upwards it is zero order since it does not depend on concentration when the catalyst is operating at full capacity [21].

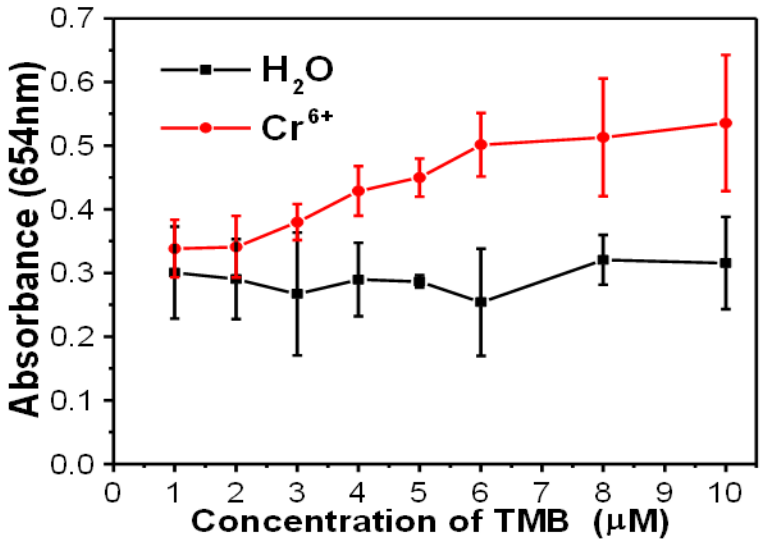


Fig 3.6 the impact that concentration of TMB has on the absorbance intensities of a reaction system containing an acetate buffer (pH 4), 1, 2, 3, 4, 5, 6, 8 and 10 mM TMB, deionized water or 100 µM Cr^{6+} after 5 min incubation time.

3.3.4 Steady-state kinetic assay

The kinetics study as described in **section 3.2.13** closely resembled the Michaelis- Menten model **Fig 3.7a** and its double reciprocal which is the Lineweaver- Burk plot (**Fig 3.7b**) allowed us to obtain the kinetics parameters such as the Michaelis- Menten constant (K_m) and maximal reaction velocity (V_{max}). The K_m value allows us to comment on the binding affinity of the particles with regard to chromium (VI) and since we obtained a low value of 0.2889 mM, we can conclude that there is high binding affinity between the two. The Beer-lambert law (A = εbC) allowed for estimation of the initial rates of catalytic reactions, taking the molar absorptivity of oxTMB (39,000 $M^{-1} \cdot cm^{-1}$) [33]. The maximum reaction velocity allows us to comment on the enzymatic activity of the particles in the presence of chromium (VI) and the high value of 2.82×10^{-7} $M.s^{-1}$ indicates that there is high enzymatic activity when the analyte is present.

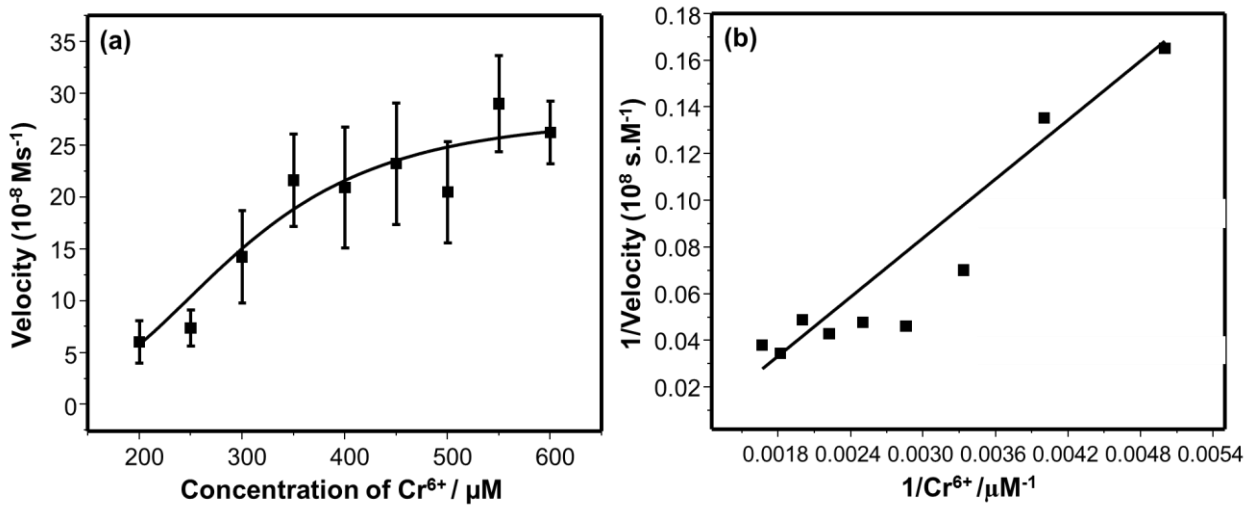


Fig 3.7: (a) Steady state kinetic study of CuS/Fe_3O_4 using different concentrations of chromium (VI) and fixed concentration of TMB (b) The corresponding Lineweaver-Burk plot.

3.3.5 Sensitivity and selectivity of the method

Reaction mixtures containing CuS/Fe_3O_4, TMB and distinct concentrations of Cr (VI) proved that the absorbances obtained depends on the concentration of chromium (VI). **Fig 3.8a** it is clear that as the concentration of chromium (VI) is increased, the absorbance is also increased. The intensity of the absorbance keeps increasing gradually with concentration resulting in a wide linear range of 0 – 1500 µM with an equation of y = 0.0015x + 0.188 (R^2= 0.9928). The detection limit equation, 3σ/S was employed and gave LoD of 0.060 µM (σ from the equation is the error of the slope and S is the slope of the line). The maximum chromium (VI) concentration allowed in industrial and domestic waste water by the WHO is 10 µM and the LoD for our method is much lower than that [114]. The advantages of our method over other methods of the enzyme mimic activity include the fact that it is cost- effective, rapid and environmental friendly since it uses a green oxidant oxygen in place of the highly unstable hydrogen peroxide. Its broad linear range makes it applicable over a wide range of concentrations of Cr (VI). **Table 3.1** shows methods reported for the detection of chromium (VI) using different nanomaterials possessing the enzyme mimic activity.

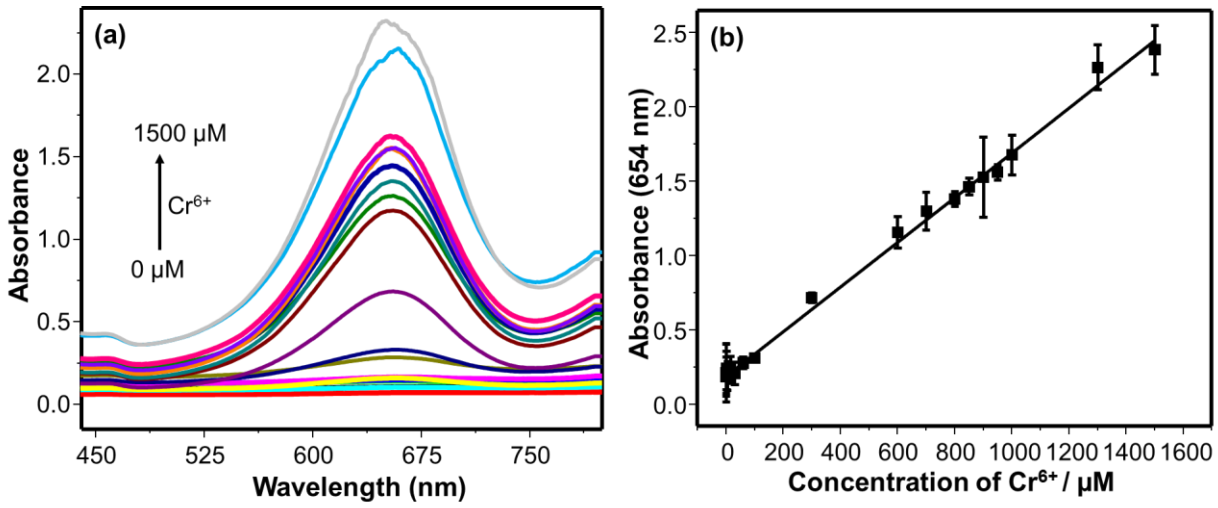


Fig. 3.8. (a) UV/ Visible absorption spectra of oxTMB for varying concentrations of chromium (VI) (b) Concentration-response plot corresponding to the spectra. The reaction systems contain an acetate buffer (pH 4), 6 mM TMB, 2.5 mg of CuS/Fe_3O_4 and various concentrations of chromium (VI) incubated for 5 min.

Table 3.1: Comparison of the present method with other reported peroxidase-like colorimetric methods.

No	Nanomaterial (Enzyme-like activity)	Limit of detection (µM)	Linear range (µM)	Reference
1.	Au-Hg amalgam	0.00071	0.001-2	[15]
2.	PEI-AgNCs	1.10	5-100	[34]
3.	Au-Ag/L-Cys-rGO	26.39	0 -200	[35]
4.	rGO/PEI/Au	0.00214	0.005-10	[36]
5.	CuS/Fe_3O_4	0.060	0-1500	This work

The spectra and the bar graph (**Fig. 3.9a, b**) shows us that only in the presence of chromium (VI) and MnO_4^- is the oxidation of TMB initiated and hence changing its color from colorless to blue indicating the formation of oxTMB with a peak for absorption at 654nm. In the presence of other

metal ions and anions, the absorbance obtained is negligible since it is the same as the one for the control (with no ion present) which further proves that the presence of chromium (VI) enhances the oxidase- mimic effect. This proves the selectivity of our method towards chromium (VI) over other anions and cations. Unlike in the cases of individual ions systems, here, there is a noticeable absorption at 654 nm for all the binary systems (**Fig. 3.9c**). This response is a result of Cr^{6+} being able to initiate oxidation of TMB thus confirming its role which is enhancing the oxidation of TMB [34] and the ability of the method to detect chromium (VI) selectively.

In the case of MnO_4^-, an immediate color change was observed proving oxidation of TMB in the absence of the nanocomposite (**Fig. 3.9d**). This proves direct oxidation of TMB by MnO_4^- in the absence of a catalyst [37].

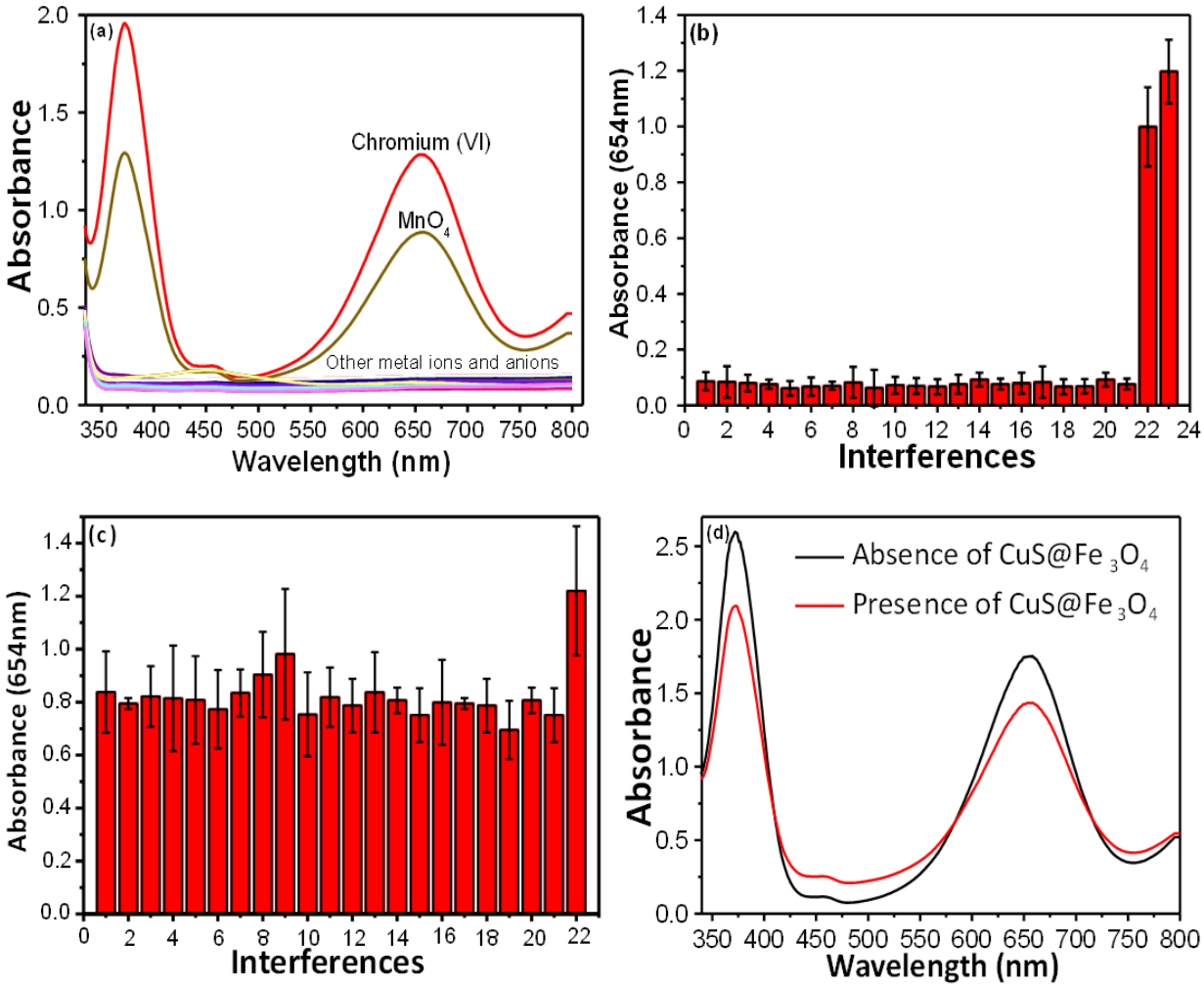


Fig. 3.9. (**a**) UV/visible absorption spectra for reaction solutions (2.5 mg of CuS/ Fe_3O_4, acetate buffer of pH 4.0, 6mM TMB) in the presence of interfering metal ions and anions after incubation for 5 min. (**b**) The corresponding bar graph showing absorbance intensities at 654 nm (1-H_2O; 2-Ag^+; 3-Ba^{2+}; 4-Ca^{2+}; 5-Co^{2+}; 6-Cr^{3+}; 7-Cu^{2+}; 8-Fe^{2+}; 9-Fe^{3+}; 10-Hg^{2+}; 11-K^+; 12-Mg^{2+}; 13-Na^+; 14-Ni^{2+}; 15-Pb^{2+}; 16-Zn^{2+};17-NO_3^-; 18-Cl^-; 19-SO_3^{2-}; 20-NO_2^-; 21-SO_4^{2-}; 22-MnO_4^-; 23-Cr^{6+}). (**c**) Bar graphs for absorbance intensities at 654nm for binary systems (1-H_2O/ Cr^{6+}; 2-Ag^+/ Cr^{6+}; 3-Ba^{2+}/ Cr^{6+}; 4-Ca^{2+}/ Cr^{6+}; 5-Co^{2+}/ Cr^{6+}; 6-Cr^{3+}/ Cr^{6+}; 7-Cu^{2+}/ Cr^{6+}; 8-Fe^{2+}/ Cr^{6+}; 9-Fe^{3+}/ Cr^{6+}; 10-Hg^{2+}/ Cr^{6+}; 11-K^+/ Cr^{6+}; 12-Mg^{2+}/ Cr^{6+}; 13-Na^+/ Cr^{6+}; 14-Ni^{2+}/ Cr^{6+}; 15-Pb^{2+}/ Cr^{6+}; 16-Zn^{2+}/ Cr^{6+}; 17-NO_3^-/ Cr^{6+}; 18-Cl^-/ Cr^{6+}; 19-SO_3^{2-}/ Cr^{6+}; 20-NO_2^-/ Cr^{6+}; 21-SO_4^{2-}/ Cr^{6+}; 22-MnO_4^-/ Cr^{6+} (**d**) The UV/ Visible spectra of the reaction systems in the presence and absence of CuS/ Fe_3O_4 after incubation of 5min.Error bars indicate standard deviations (n = 3).

3.3.6 Determination of Cr^{6+} in tap water

Fig. 3.10 shows the absorbance against concentration plots for both deionized water and tap water for analyzing chromium (VI). From the plots it is evident that whether we use deionized water or tap water, there is no noticeable difference in the responses obtained suggesting that our method is capable of determining chromium (VI) quantitatively in real samples. **Table 3.2** shows the recoveries calculated when the method was applied to tap water samples of different chromium (VI) concentrations. The data proves the applicability of the method to real sample analysis with percentage recoveries ranging from 97-110%.

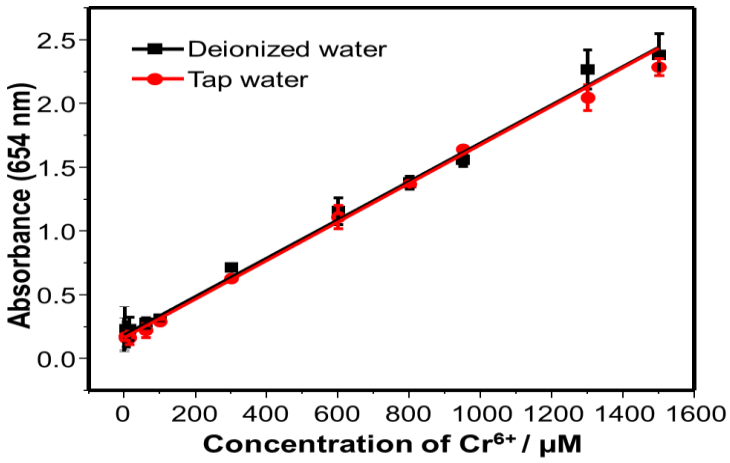


Fig. 3.10. Increase in absorption intensities at 654nm (2.5 mg CuS/ Fe_3O_4, acetate buffer of pH 4.0, 6 mM TMB) when the concentration of Cr^{6+} in tap water is increased.

Table 3.2: Recoveries obtained after analyses of chromium (VI) in tap water by use of this method.

Tap water (%)	Prepared Cr^{6+} (µM)	Obtained (µM)	Percentage recovery
1.	15.00	16.56 ± 0.01	110.38
2.	300.00	291.83 ± 0.05	97.28
3.	600.00	611.04 ± 0.08	101.84

3.4 Summary

A simple hydrothermal method was used to prepare the CuS/Fe_3O_4 nanocomposites possessing the oxidase-like property that was employed for detection of Cr^{6+} exploiting the oxidation reaction existing between Cr^{6+} and TMB. This method does not incorporate the use of H_2O_2 which is unstable and environmentally unfriendly and the CuS/ Fe_3O_4 nanocomposites can be recovered using a magnet thus making the method environmentally friendly. The use of H_2O_2 compromises the repeatability and reproducibility of a method and since this method does not incorporate it, it avoids that compromise. It is affordable as compared to other methods which use big and expensive instruments that need specific rooms to accommodate them and only specialized operators. Even in the presence of other interfering metal ions and anions, this method has proved to be selective and sensitive of Cr^{6+}. It was applied in the detection of Cr^{6+} in tap water and proved to be applicable to real sample analysis.

CHAPTER 4: Colorimetric detection of chromium (VI) via its instigation of oxidase-mimic activity of CuO

4.1. Introduction

Industrialization has not come entirely with the benefit of human beings; it is accompanied by pollution. Unfortunately, the waste in industries usually finds a way into water sources [115]. Extensive use of chromium in leather tanning, electroplating, textile dyeing, and mining activities, makes chromium among the major pollutants that is discharged to water sources [116]. Chromium has various oxidation states, and the hexavalent state, chromium (VI), is toxic and has detrimental health effects [117]. Because of its excessive toxicity a permissible concentration limit of chromium (VI) in water has been recommended. The US Environmental Protection Agency (USEPA) recommended 0.05 mg/L as the maximum permissible Cr (VI) concentration in drinking water. The concentration in the final disposal of wastewater to the environment is however 0.10 mg/L [118]. This necessitates methods for quantification of chromium (VI) in water to ensure that the concentrations in drinking water and wastewater are within the permitted limit and hence avoid it being consumed by humans and animals.

Atomic absorption and emission spectroscopies are usually used as sensitive techniques for detection of chromium (VI) [119], [120]. The requirement of skilled personnel for operation of the instrument and the high cost makes routine utilization of these techniques for analysis of Cr (VI) challenging [121]. Alternatively, colorimetric methods using UV/visible spectroscopy have been used for analysis of chromium (VI) [59], [122], [123]. The methods include the localized surface plasmon resonance (LSPR) [124], [125], [126], organic compounds via coordination [122], and catalytic based [114], [127], [128]. Generally, colorimetric methods have attractive properties including simplicity, low cost, rapid signal readout, and possibility of onsite analysis [129]. However, colorimetric methods that produce signals based on LSPR and coordination organic compounds formation [with target analyte], have limitations. For example, the LSPR method requires careful preparation, size and shape control, and modification of plasmonic nanoparticles to produce the signal readout [129]. The low stability of the colloidal nanoparticles is also prone to aggregation that can deter signal production for long term application. Generally, the LSPR based colorimetric detection requires careful inquiry of analyte-particle interaction or modification of the plasmonic nanoparticles for meaningful signal production [130]. Utilization of organic compounds for formation of coordination organic compounds to produce signal makes

colorimetric method based on coordination unsafe and environmental unfriendly. Catalytic based colorimetric methods, on the other hand, use catalytic reaction of a single product molecule [131], or chromogenic substrates such as OPD, TMB, and ABTS to produce a signal readout for detection of target analytes. The principle in nanozymes-based colorimetric strategy is via inhibiting or enhancing the signal produced by the catalytic reaction with the target analyte. The response that corresponds to the concentration of the target analyte can be investigated colorimetrically.

Nowadays, nanomaterials with various enzyme-mimic activities including oxidase, peroxidase, and laccase for detection of different analytes have been reported [132], [133]. Heavy metal ions are among the analytes that are detected basing on the enzyme-mimic activities of various nanomaterials [134]. In this regard application of plasmonic nanomaterials as enzyme-mimic activities for analyses of chromium (VI) have received great attention [59], [55], [114], [127]. The methods are sensitive and enable selective determination of chromium (VI). The plasmonic nanomaterials are, however, expensive that needs alternative cheap nanomaterials. Copper based nanomaterials are good candidates in this regard and they exhibit enzyme-mimic activity with different applications including sensing. For example, Chen *et al.,* [33] demonstrated the peroxidase-like activity of copper oxide using 2,2′-azino-bis (3-ethylbenzothiazoline-6-sulfonic acid) diammonium salt (ABTS), 3,3′-diaminobenzidine (DAB) and TMB as peroxidase substrates a decade year back. The tandem nanozymes activity of CuO as recently demonstrated by He *et al.,* [135] and its stability in a wider range of pH and temperature [136] show the capacity of CuO in sensor development. Fast interfacial electron transfer, excellent stability and high electrocatalytic activity in some redox reactions are additional advantages of CuO [137]. Inspired by this, CuO nanoparticles with enzyme-mimic activity was prepared for analysis of chromium (VI).

In this assay, a simple hydrothermal method was used to prepare the CuO. In the presence of chromium (VI), CuO nanoparticles exhibited a pronounced catalytic activity using TMB as chromogenic substrate. The enzyme- mimic activity of CuO has been used to detect various analytes but to our knowledge, this is first assay that applies to detection of chromium (VI) [33], [135], [136], [137]. The method avoids utilization of the unstable and environmental unfriendly H_2O_2 as oxidizing agent. Importantly, this study reports utilization of relatively non-expensive and stable material for detection of chromium (VI) in contrast to expensive plasmonic

nanostructures that were used for analysis of chromium (VI) *via* oxidoreductase activity [47], [59], [114]. Moreover, the particles exhibit enzyme-mimic activity in the extended range of temperature unlike natural enzymes and nanozymes.

4.2. Experimental

4.2.1. Chemicals

All reagents were of analytical grade and were used without additional purification. The analytes were prepared in Millipore double deionized water. Copper (II) nitrate trihydrate and Sodium acetate trihydrate were bought from Alpha Chemika (Mumbai, India). Potassium chloride and ferric chloride were purchased from Associated Chemical Enterprise (ACE) (Johannesburg, RSA). Sodium nitrite, Mercuric sulphate, Potassium permanganate, chromic chloride and Zinc nitrate hexahydrate were purchased from MERCK (Gauteng, RSA). Potassium dichromate and nickel sulphate were obtained from Minema (Roodeport, RSA). Silver nitrate, ethylene glycol, ferrous sulphate hydrate, calcium chloride dihydrate and sodium sulphite were purchased from Rochelle Chemicals (Johannesburg, RSA). Acetic acid and Dimethyl Sulfoxide were purchased from Sigma Aldrich (France). Magnesium acetate tetrahydrate was obtained from Sigma Aldrich (Germany). Barium chloride dihydrate was from Sigma Aldrich (Japan). Lead (II) nitrate and Copper (II) acetate were purchased from Sigma Aldrich (St Louis, USA). TMB was purchased from Sigma Aldrich (Switzerland). Cobaltous chloride was purchased from UNIVAR (Muldersdrift, RSA).

4.2.2. Instrumentation

EDX data was obtained using an energy-dispersive spectrometer interfaced with the FE-SEM. A field emission scanning electron microscope (FE-SEM, JSM-7100F, JEOL Ltd., Tokyo, Japan) was used to collect the SEM image at an accelerating voltage of 10 kV. The TEM image was obtained using transmission electron microscopy (TEM, JEOLJEM-200 EX). UV/Visible absorption spectra's were obtained using a Thermo-Fischer UV/Visible spectrophotometer (Evolution 201, Shanghai, China). X-ray diffraction (XRD) spectrum was collected using D2 phaser XRD-300W powder diffractometer (Bruker, AXS GmbH, Karlsruhe, Germany). Cu Kα radiation at 40 kV of 100 mA for a 2θ range of 20° to 80° at a scan rate of 0.05°/s was used as a radiation source.

4.2.3. Preparation of the copper oxide nanoparticles

The copper oxide nanoparticles were synthesized following a hydrothermal method as reported by Wang *et al.* [138] with slight modifications. Briefly, 0.25 g of copper acetate and 2.7 g of sodium acetate were added to a 25 mL solution of ethylene glycol and water of 1:4 ratio and magnetically stirred until homogeneous solution was formed. The homogenous solution was transferred to a Teflon coated autoclave and placed in an oven at 160^{o}C for 10 hrs. The produced particles were washed by centrifugation using ethanol and deionized water several times then dried in an oven at 70^{o}C.

4.2.4. Preparation of solutions

Potassium dichromate stock solution (2 mM) was prepared in a 100 mL vol. flask using deionized water as the solvent. Acetate buffer (pH 4.0) was prepared using anhydrous sodium acetate (0.99g) and acetic acid (2.218 mL) and diluted to the mark with deionized water in a 250 mL volumetric flask. A 10 mM stock solution of TMB was prepared using the appropriate mass in a 25 mL volumetric flask and from it the required concentrations were prepared in 2 mL Eppendorf tubes using dimethyl sulfoxide (DMSO) as the solvent. The tubes were wrapped with aluminum foil and stored in a dark place. Buffers used to investigate the effect of pH were prepared from stock solutions of dibasic sodium phosphate and citric acid prepared in 250 mL volumetric flasks using deionized water as the solvent. The interference molecules used for selectivity study were prepared in 50 mL volumetric flasks using the appropriate masses (400 µM).

4.2.5. Enzyme-mimic activity of the CuO nanoparticles

The enzyme- mimic activity of the CuO nanoparticles was investigated based on the oxidation of TMB as the substrate. The color change of TMB from colorless to the blue (oxTMB) upon addition of Cr (VI) allowed us to investigate the enzyme- mimic activity of the nanoparticles. Reaction mixtures including TMB only; TMB, and chromium (VI); TMB and CuO; TMB, chromium (VI) and CuO (all in acetate buffer of pH 4.0) were incubated before they could be transferred to a cuvette. The mixtures were centrifuged for 30 sec at 8000 rpm to allow the nanoparticles to settle at the bottom of the Eppendorf tube and only transferring the supernatant to the cuvette so as the avoid the interference of the particles with the UV/ Visible light beam. The whole process was done under 5 min and at 5 min their absorbance was measured using a

UV/ Visible spectrophotometer from a range of 300- 800nm. The oxTMB is expected to show an intense absorption peak at around 654 nm.

4.2.6. Optimization of parameters

To come up with a sensitive method, parameters used have to give the highest absorbance and in order to obtain that a method needs to be optimized. In this assay the mass of CuO nanoparticles, pH of the buffer, concentration of TMB and temperature were optimized and the optimum values for the parameters used for further analysis.

4.2.7. Optimization for mass

To a 2 mL Eppendorf tube containing different masses of CuO (1.0 to 3.0mg), 1.6 mL of acetate buffer (pH 4.0), 200 µL of 6 mM TMB and 200 µL of 400 µM of Cr (VI) or DI water for the control were added and incubated for 5 min on a shaker. Within the 5 min the mixture was transferred to a cuvette after centrifuging for 30 sec and at 5 min its absorbance was measured. The measurement for each mass was repeated three times and the average used for comparison with the others in order to determine the optimum mass.

4.2.8. Optimization for concentration of TMB

To a 2 mL Eppendorf tube 2.0 mg of CuO, 1.6 mL acetate buffer (pH 4.0), 200 µL of varied concentrations of TMB (1 to 10 mM) and 200 µL of 400 µM Cr (VI) were added and the mixture incubated for 5 min. After that, the mixture was transferred to a cuvette to measure absorbance. Each concentration of TMB was run three times.

4.2.9. Optimization for pH

Buffers of pH ranging from 3.0 to 6.6 were used to carry out this optimization study in order to determine the optimum pH. To a 2 mL Eppendorf tube containing the optimized mass of catalyst (2.0 mg), 1.6 mL of varying buffers, 200 µL of 10 mM and 200 µL of 400 µM Cr (VI) were added and the mixture incubated for 5 min before being transferred to a cuvette to measure absorbance. Buffers of different pH were used in each measurement and each pH was run three times.

4.2.10. Optimization for temperature

To a 2 mL Eppendorf tube 2.0 mg of CuO, 1.6 mL acetate buffer (pH 4.0), 200 µL of 10 mM of TMB and 200 µL of 400 µM Cr (VI) was incubated in a water bath of varying temperatures (4 to 55°C) for 5 min and its absorbance determined.

4.2.11. Colorimetric detection of chromium (VI)

The impact of dissolved oxygen was investigated by the use of scavenger molecules, p-benzoquinone ($O_2^{\bullet-}$ scavenger) and t- butanol ($^{\bullet}OH$ scavenger) with DI as the control. Mixtures containing the CuO (2.0 mg), 100 µL of DI water or p- benzoquinone (20 µM) or t- butanol (10 mM), 1.6 mL acetate buffer (pH 4.0), 200 µL of TMB (10 mM) and 100 µL of 400 µM chromium (VI) were incubated for 5 min and their absorbances measured and compared.

The detection of Cr (VI) was done by placing 2.0 mg of CuO in a 2 mL Eppendorf tube and adding 1.6 mL of acetate butter (pH 4.0), 200 µL of 10 mM TMB and 200 µL of 400 µM Cr (VI) or DI water as the control. The mixture was incubated for 5 min before measuring its absorbance using a UV/ Vis spectrophotometer using the absorption range from 300 to 800 nm.

4.2.12. Steady state kinetics study

The kinetics study was performed by following the optimized conditions with varying concentrations of TMB (0.1 to 0.5mM) and 200 µL of 400 µM Cr (VI). The absorbances for each concentration were recorded at different time intervals until the absorbance became constant. The absorbance (654 nm) against time graphs were plotted for each concentration of TMB and by employing the Beer Lambert's law, the initial velocities were estimated and plotted against concentration of TMB (Michaelis- Menten curve). The Lineweaver- Burk plot was used to calculate the kinetics parameters V_{max} and K_m. **See detailed explanation in section 3. 2. 13.**

4.2.13. Sensitivity

Using the procedure for colorimetric detection of Cr (VI) and the optimized conditions, the sensitivity of the method was investigated. The concentration of Cr (VI) was varied from the lowest (0.0 µM, which is basically DI water) to 1050 µM. Each concentration was run three times and the average absorbance used to plot the calibration curve which involved the concentrations that made a linear plot with the highest R^2 value (0.1 to 650 µM). The calibration curve therefore allowed for the calculation of the limit of detection (LoD) and limit of quantification (LoQ).

4.2.14. Selectivity

The selectivity study followed the procedure for detection of Cr (VI). In this case 200 µL of 400 µM of interfering cations such as Ag^+, Ba^{2+}, Ca^{2+} Co^{2+}, Cr^{3+}, Cr^{6+}, Cu^{2+}, Fe^{2+}, Fe^{3+}, Hg^{2+}, K^+, Mg^{2+}, Na^+, Ni^{2+}, Pb^{2+}, Zn^{2+}, and anions such as NO_3^-, NO_2^-, SO_3^{2-}, SO_4^{2-}, $MnO4^-$, and Cl^- were

used in place of Cr (VI). Chromium (VI) was also included for comparison. Each interference was run three times and the average absorbances were compared using bar graphs. A binary mixture which involved 100 µL of 400 µM for both Cr (VI) and the interference was also studied to investigate the sensitivity of the method for Cr (VI) even in the presence of the interference.

4.2.15. Real sample analysis

A 2 mM stock solution of potassium dichromate was prepared using tap water as the solvent in a 100 mL volumetric flask. Working standards of different concentrations of Cr (VI) were prepared from the stock in 2 mL Eppendorf tubes filling to the appropriate volumes with tap water. The analysis was done following the same procedure as that of sensitivity with each concentration being run three times.

4.3. Results and discussion

4.3.1. Characterization of CuO

A simple hydrothermal method was used to prepare CuO nanoparticles. The resulting particles were characterized by EDX, SEM, XRD and TEM. The purity and phases of the particles were investigated by XRD. The XRD spectrum is given in **Fig. 4.1a**. The diffraction peaks are observed at 2θ angles of 29.58, 32.52, 35.52, 36.44, 38.74, 42.32, 48.80, 53.47, 58.26, 61.47, 66.18, 67.92, 73.52, 75.06, and 78.80°. The peaks are attributed to (110), (110), (-111), (002), (111), (200), (-202), (020), (202), (-113), (311), (113), (311), (004) and (222) planes respectively [139]. The SEM and TEM images revealed irregular shaped particles with no significant variation in sizes (**Fig. 4.1b & c**). The weight percentage composition of the particles from EDX shows that 78.01 and 21.99% of the particles constitute copper and oxygen respectively.

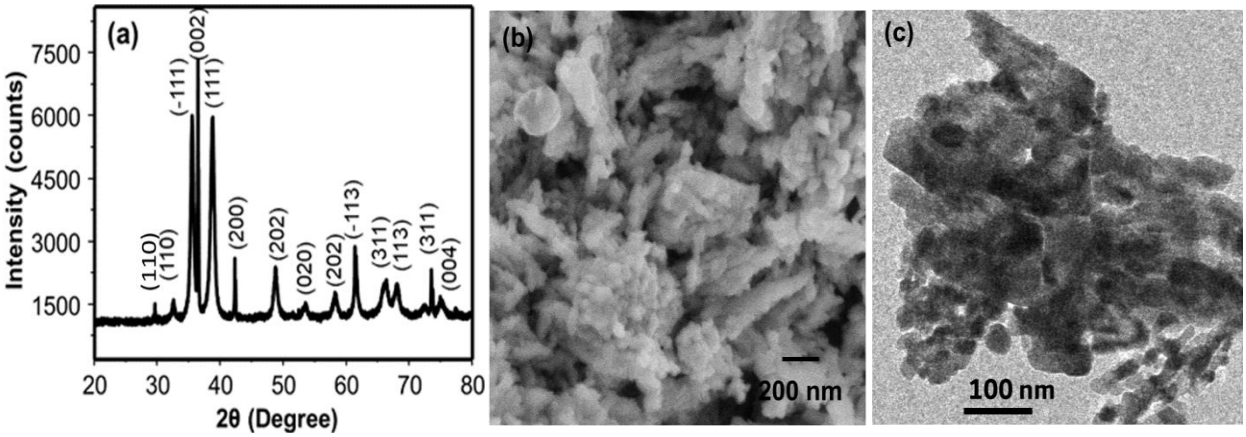


Fig. 4.1 (**a**) The XRD spectrum of CuO; (**b**)SEM image of CuO; (**c**) TEM image of CuO.

4.3.2. Chromium (VI) as an initiator of enzyme-mimic activity of CuO

The enzyme-mimic activity of the produced CuO particles was evaluated by considering different conditions. The colorless TMB solution remained unchanged that reveals non-existence of oxidation of TMB (**Fig. 4.2a**) (**black curve**). Oxidation of TMB (in acetate buffer) was slightly pronounced in the presence of chromium (VI) as witnessed from the absorption spectrum (**red curve**) showing that the presence of Cr (VI) triggers oxidation of TMB. The colorless TMB solution remains unchanged also in the presence of CuO alone and acetate buffer (**green curve**). The introduction of the CuO nanoparticles, however, has the colorless TMB solution changing color to the deep blue oxTMB. These observations show that the enzyme-mimic activity of CuO can be observed in the presence of chromium (VI).

An increment in absorbance is observed as the mass of CuO increased from 1 mg to 1.5 mg. Further increment of amount of CuO, however, did not change the catalytic activity significantly (**Fig. 4.2b**). The catalytic activity, however, remained unchanged with further increment of mass of CuO. The difference in absorption of the reaction system with and without (water as a control) chromium (VI) was used to assess the response of the reaction system to chromium (VI). Regardless of the mass of the catalyst, the CuO particles showed no catalytic activity in the absence of Cr (VI). **Fig 4.2c** shows that absorbance increases with increase in concentration of TMB from 1 mM to 10 mM proving that the reaction is 1st order since it is dependent on concentration. The highest concentration (10 mM) became the optimum concentration of TMB since it gives the highest absorbance.

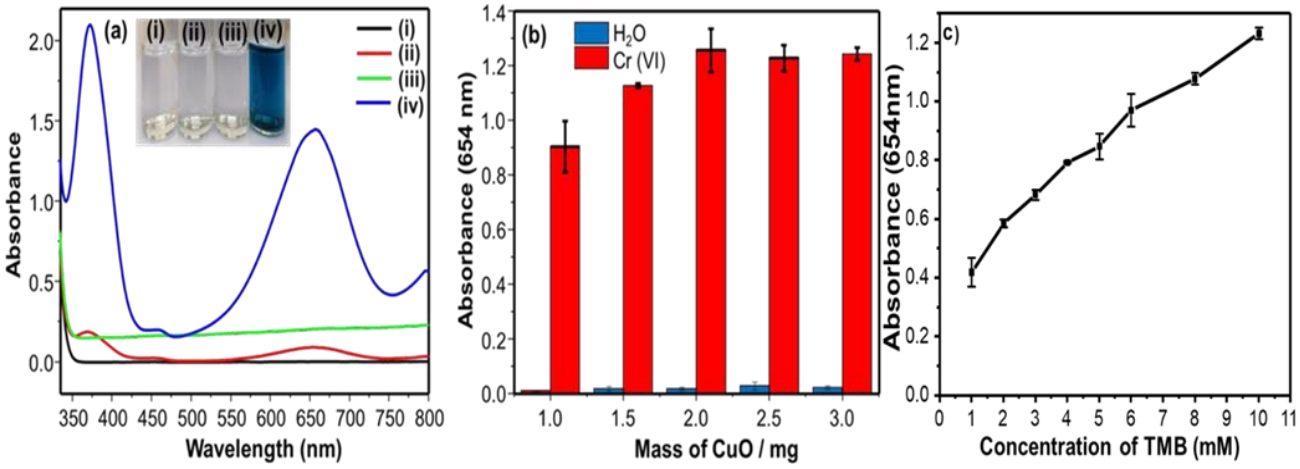


Fig. 4.2 (**a**) UV/ visible absorption spectra obtained from TMB for different reaction conditions: (i) TMB only; (ii) TMB and chromium (VI); (iii) TMB and CuO; (iv) TMB, CuO and chromium (VI). (**b**) Bar graph showing absorption intensities of oxTMB of different amount of CuO, 1.6 mL acetate buffer of pH 4.0 and 6 mM TMB in the presence and absence of 400 µM Cr (VI) (**c**) line graph depicting the absorption intensities of oxTMB using different concentrations of TMB (1 to 10 mM).

4.3.3. Factors affecting the enzyme-mimic activity of CuO

Oxidation of TMB took place well in all tested buffers (**Fig. 4.3a**). The reaction mixtures containing buffer of low pH exhibited relatively higher activities. This behavior may be associated with formation of positively charged TMB [140]. Further increment of the pH reduces the catalytic activity as reflected from the absorption intensities. Temperature-controlled water bath was used to investigate the effect of temperature on the catalytic activity of CuO. The reaction temperature ranging from 4^{o}C to 55^{o}C were investigated. The results show that (**Fig. 4.3b**), there is no noticeable difference in the catalytic activity of the studied temperature. Interestingly, the catalytic activity is not less for the reaction system at 4^{o}C. This reveals the capacity of the produced CuO in catalyzing the oxidation of TMB favorably at lower and higher temperature. This gives an opportunity to apply the assay within the mentioned temperature range.

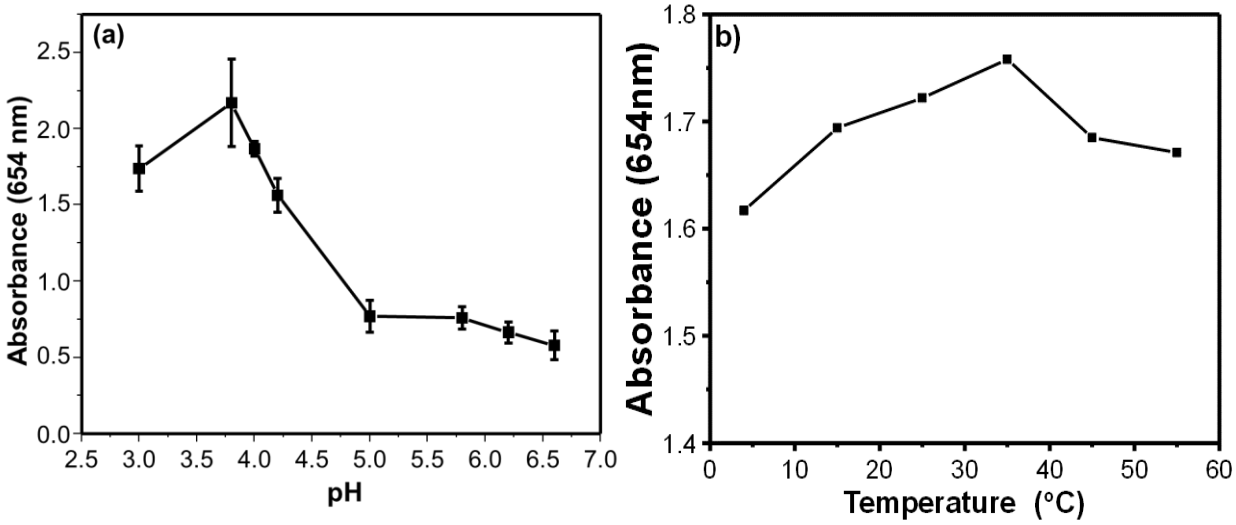


Fig. 4.3 Effect of pH (**a**) and temperature (**b**) on the enzyme-mimic activity of CuO.

4.3.4. Catalytic reaction mechanism

The nature of the reactive oxygen species (ROS) was assessed to investigate the mechanism of the catalytic reaction. The free radical quenching molecules were used to study the involvement of ROS in the catalytic reaction. T- butanol and *P*-benzoquinone were used as superoxide ($O_2^{\bullet -}$) and hydroxyl ($^{\bullet}OH$) free radical scavenger respectively [128], [141]. In a typical reaction mixture, 2 mg of CuO, acetate buffer, TMB, chromium (VI), and *t*-butanol or *p*-benzoquinone or H_2O (as a control) were mixed and incubated on a shaker. After incubating the reaction mixtures for 5 min, the UV/visible measurements were done. The reaction system with *t*-butanol, showed no difference with that of the reaction mixture containing H_2O as presented in **Fig. 4.4**. This reveals the fact that *t*-butanol did not obstruct the oxidation of TMB such that the reaction did not proceed *via* $^{\bullet}OH$ free radical. However, in the presence of p-benzoquinone the absorbance intensity decreased drastically confirming obstruction of oxidation of TMB. In other words, the ROS, which is $O_2^{\bullet -}$ may be scavenged by *p*-benzoquinone and the oxidation of TMB that may use $O_2^{\bullet -}$ as an electron donor may be blocked. The large difference between absorption intensity at 654 nm of oxTMB for H_2O and *p*-benzoquinone confirms the involvement of $O_2^{\bullet -}$ in the oxidation of TMB. Thus, we can conclude that CuO and chromium (VI) activates O_2 to $O_2^{\bullet -}$ and resulted in rapid oxidation of TMB [142], [143].

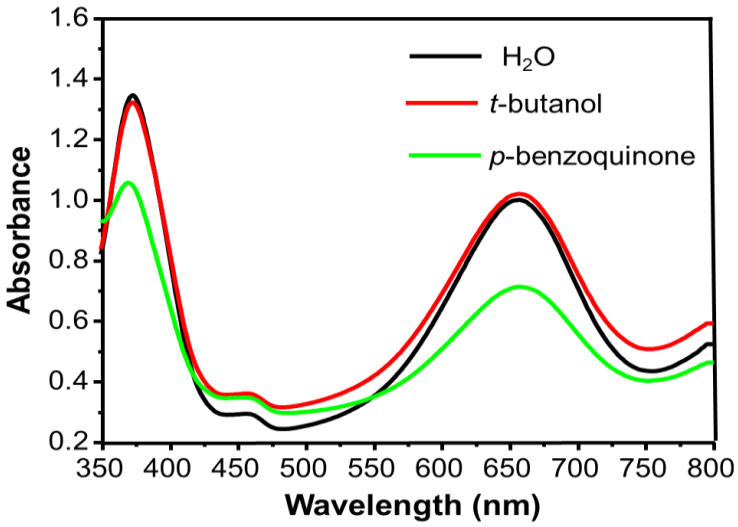


Fig. 4.4 Effect of *t*-butanol and *p*-benzoquinone on oxidation of TMB. The reaction systems contain 2 mg of CuO, 1.6 mL of acetate buffer, 200 µL of 10 mM TMB, 100 µL of 400 µM chromium (VI), and 100 µL of H_2O (control), or 10 mM *t*-butanol, or 20 µM *p*-benzoquinone incubated for 5 min.

4.3.5. Steady-state kinetic study

The kinetic study was further done to explore the enzyme-mimic activity of CuO particles. The Michaelis-Menten curves (**Fig. 4.5a**) and the double reciprocal of the Michaelis-Menten curve (**Fig. 4.5b**) (Lineweaver- Burk plot) were computed and the kinetic parameters such as the maximum reaction velocities (V_{max}) and Michaelis constant (K_m) were obtained. These parameters assist to predict the affinity and enzymatic activity of the particles [58], [144]. Relatively strong binding affinity of the particles towards TMB was observed as demonstrated from the lower K_m value of 1.097 mM [144]. The V_{max} was obtained as 1.989 mM/min which shows that the particles had high enzymatic maximal reaction activity in the presence of TMB.

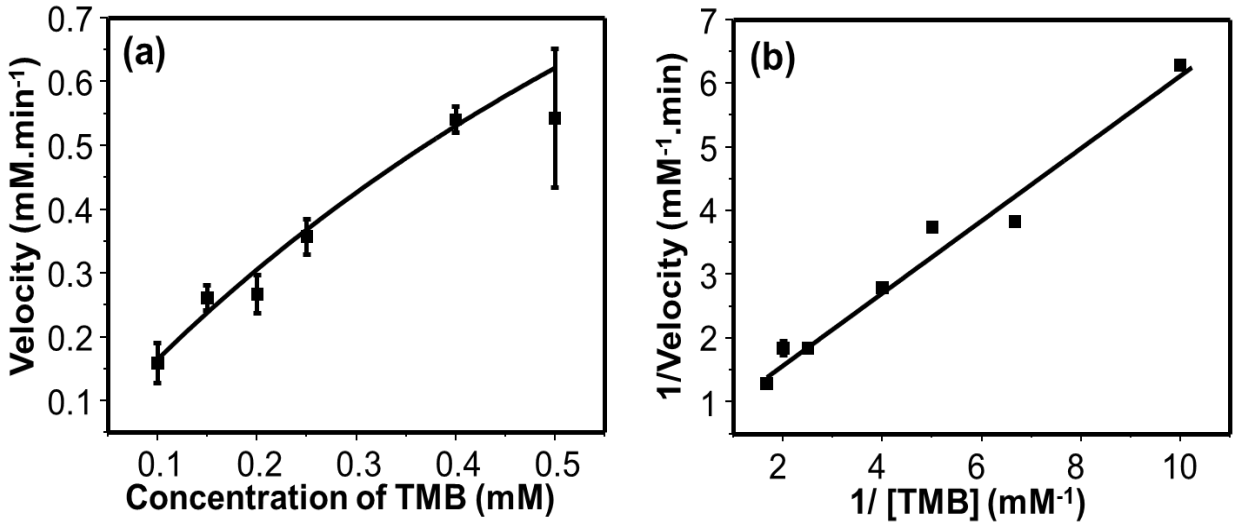


Fig. 4.5 (**a**) The Michaelis-Menten curve for TMB and (**b**) the corresponding Lineweaver-Burk plot.

4.3.6. Sensitivity and selectivity of the method for determining chromium (VI)

We observed that the catalytic activity of CuO is dependent on the concentration of chromium (VI). Taking this advantage a colorimetric method for detection of chromium (VI) was developed. Under optimum conditions, chromium (VI) concentrations ranging from 0.1 to 950 µM were prepared and used for UV/visible spectroscopy measurements after incubation for 5 min. The absorption intensities increase with increment in concentration of chromium (VI). The spectra and the corresponding concentration profile curve are given in **Fig. 4.6a & b**. The concentration profile curve is linearly fitted in the range of 0.1-650 µM with regression line of equation, $y = 0.0027x + 0.0262$ ($R^2 = 0.993$) (**Fig. 4.6b** insert). The regression line is used to estimate the limit of detection (LoD) using $3\sigma/S$, with S being the slope of the regression line and

σ the standard deviation of the slope and the limit of quantification (LoQ) using 10σ/ S. The LoD and LoQ are found to be 0.079 and 0.264 µM respectively. Both the LoD and LoQ are well below the threshold set by WHO for concentration of chromium (VI) in drinking and industrial water [114]. This shows the high sensitivity of the method in quantification of Cr (VI) in water. On **Table 4.1**, different methods based on peroxidase-like activity for quantification of chromium (VI) are reported. The results show that our method is either better or closer with respect to LoD.

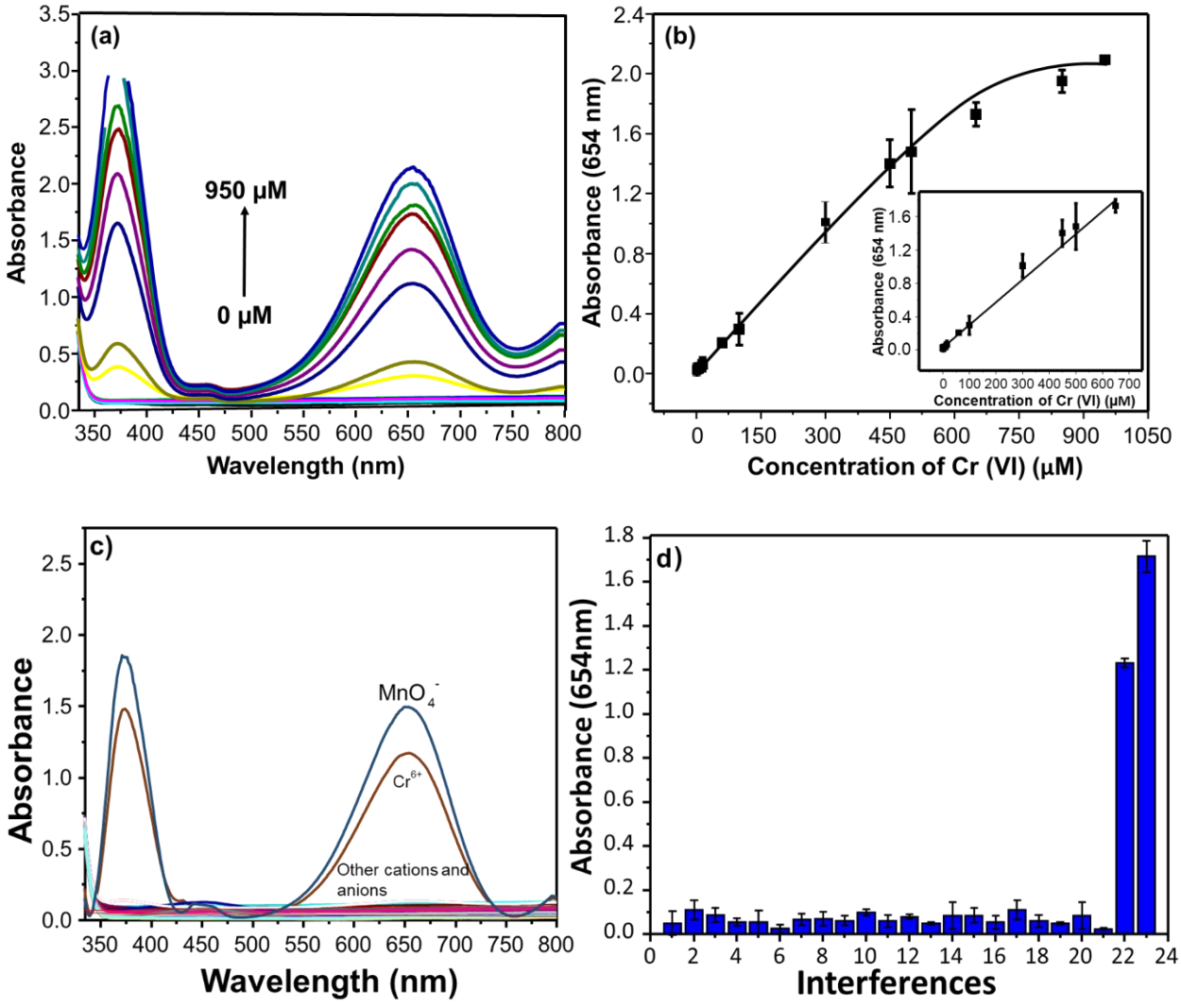


Fig. 4.6 (**a**) UV/visible absorption spectra of oxTMB showing the effect of concentration of chromium (VI); (**b**) Concentration profile curve for a range of concentrations of chromium (VI) (n=3); (**c**) UV/visible absorption spectra obtained from 5 min incubation of TMB, 2 mg CuO, and different anions and cations showing selectivity of the method; (**d**) Bar graph showing the

intensities of the spectra from (**c**) (n=3). The tested ions are: 1= blank, 2= Ag^{+}, 3= Ba^{2+}, 4= Ca^{2+}, 5= Co^{2+}, 6= Cr^{3+}, 7=Cu^{2+}, 8=Fe^{2+}, 9=Fe^{3+}, 10= Hg^{2+}, 11= K^{+}, 12= Mg^{2+}, 13= Na^{+}, 14= Ni^{2+}, 15= Pb^{2+}, 16= Zn^{2+}, 17= NO_3^{-}, 18= Cl^{-}, 19= NO_2^{-}, 20= SO_4^{2-}, 21= SO_3^{2-}, 22= Cr^{6+} and 23= MnO_4^{-}.

Table 4.1. Comparison between the LoD and linear range of this method and those of other methods reported based on enzyme-mimic activities.

No	Nanomaterial (Enzyme-like activity)	Limit of detection (μM)	Linear range (μM)	Reference
6.	BSA- AgNCs	0.01	0.03- 0.225	[37]
7.	MOF- 199	0.02	0.1- 30	[40]
8.	Cc- AgNPs	0.0534	0- 4.2	[41]
9.	AgNPs@ Fe_3O_4	0.087	0- 20	[42]
10.	Fe_3O_4	3.0	5- 100	[43]
11.	CuO	0.079	0.1-650	This work

The selectivity of the method for chromium (VI) over other cations and anions was investigated using two approaches. **Fig. 4.6c** demonstrates that chromium (VI) prompts the oxidation of TMB and that confirms high selectivity of the method to chromium (VI). As for the binary mixture oxidation of TMB took place readily (**Fig. 4.7**). This proved that oxidation of TMB using CuO as an enzyme-mimic catalyst is promoted preferentially with chromium (VI) present. The strange response from MnO_4^{-} was discussed in the previous assay.

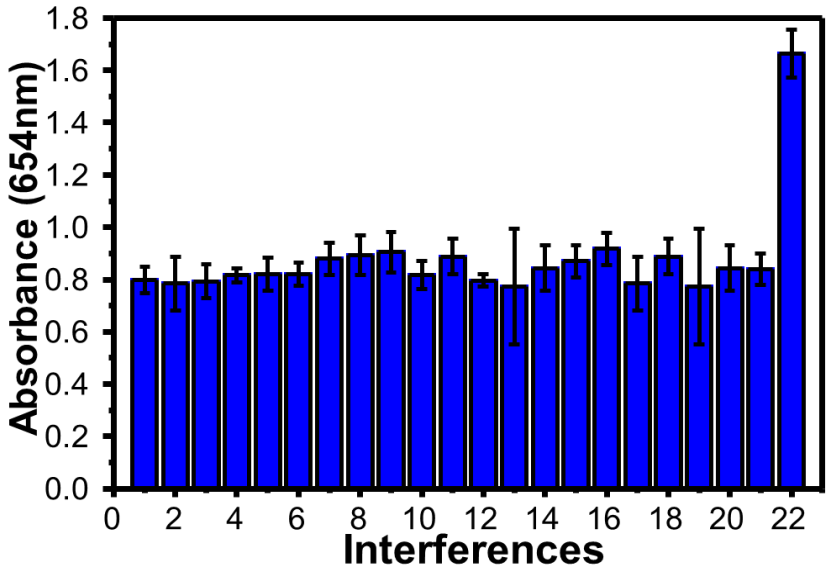


Fig. 4.7 Bar graph depicting the absorbances obtained from binary mixtures of chromium (VI) and different cations and anions (n=3). The tested ions are: 1= blank, 2= Ag^{+}, 3= Ba^{2+}, 4= Ca^{2+}, 5= Co^{2+}, 6= Cr^{3+}, 7=Cu^{2+}, 8=Fe^{2+}, 9=Fe^{3+}, 10= Hg^{2+}, 11= K^{+}, 12= Mg^{2+}, 13= Na^{+}, 14= Ni^{2+}, 15= Pb^{2+}, 16= Zn^{2+}, 17= NO_3^{-}, 18= NO_2^{-}, 19= Cl^{-}, 20= SO_3^{2-}, 21= SO_4^{2-}, and 22= MnO_4^{-}.

4.3.7. Analysis of chromium (VI) in tap water

The applicability of the method to determination of chromium (VI) in real sample was tested using tap water collected from the chemistry laboratory where the experiments were done. After it was filtered, the tap water was used for preparation of solutions of chromium (VI). The same procedure that was used for determination of chromium (VI) in deionized water was employed. The absorption measurement results revealed that the trend for the response of the reaction mixture to chromium (VI) is similar with that of the standard solutions. This shows that our method is capable of quantifying chromium (VI) in real samples. The percentage recoveries for detection of chromium (VI) in tap water are given in **Table 4.2**. The percentage recoveries range from 100% to 106% and that shows the applicability of the method in quantification of chromium (VI) in real samples.

Table 4.2. Percentage recoveries obtained from use of tap water.

Tap water	Prepared Cr^{6+} (µM)	Obtained (µM)	Percentage recovery (%)

1.	60	60.51	100.84
2.	300	319.60	106.84
3.	600	615.45	102.57

4.4. Summary

A highly selective and sensitive method for quantification of chromium (VI) was developed based on the oxidase- mimic activity of copper oxide. With Cr (VI) present, the oxidase- mimic activity of CuO nanoparticles using TMB as a substrate was initiated hence creating an opportunity for quantification of chromium (VI). The method avoids utilization of hydrogen peroxide. This makes the detection system simple. The recoveries results obtained in analysis of chromium (VI) from tap water demonstrate the applicability of our method in real sample analyses. This also shows the potential of our method to be employed in analysis of chromium (VI) in different environmental samples.

CHAPTER 5: Conclusion

Copper- based nanoparticles were prepared by a hydrothermal method and characterized using SEM, EDX and XRD. The particles proved to possess oxidase- mimic activity that was applied to detect chromium (VI) referencing to the oxidation of TMB when it is present. Under optimized conditions, the methods proved to be sensitive and selective of Cr^{6+} even among other interfering ions. A broad linear range of 0- 1500 µM and a detection limit of 0.060µM were obtained in the presence of CuS/Fe_3O_4 nanocomposites and a linear range of 0- 650 µM and detection limit of 0.079 µM were obtained in the presence of CuO nanoparticles. These limits of detection are lower than the threshold set by WHO of 10µM. The methods proved to be applicable to real sample analysis when applied to tap water. These methods have proved to be easy to perform, environmental friendly, rapid and capable of on- site analysis when compared to other methods used for detection of chromium (VI).

REFERENCES

[1] M. M. Zeitoun and E. S. E. Mehana, Impact of water pollution with heavy metals on fish health: Overview and updates, Glob. Vet., 12, 2 (2014) 219–231.

[2] S. Tabari *et. al.*, Heavy metals (Zn , Pb , Cd and Cr) in fish ,water and sediments sampled form Southern Caspian Sea , Iran, Toxicol. Ind. Health., 26, 10 (2010) 649-656.

[3] J. I. Allen and M. N. Moore, Environmental prognostics: Is the current use of biomarkers appropriate for environmental risk evaluation?, Mar. Environ. Res., 58, 2–5 (2004) 227–232.

[4] G. O. Oze *et. al.*, Metal pollution of fish of qua-iboe river estuary: Health implications, 24, 2 (2009) 1–5.

[5] R. Ouyang *et. al.*, Flower-like self-assembly of gold nanoparticles for highly sensitive electrochemical detection of chromium (VI), Anal. Chim. Acta., 722 (2012) 1–7.

[6] H. Luo *et. al.*, Chromium (IV)-mediated fenton-like reaction causes DNA damage: Implication to genotoxicity of chromate, Ann. Clin. Lab. Sci., 26, 2 (1996) 185–191.

[7] X. Shi *et. al.*, Reduction of chromium (VI) and its relationship to carcinogenesis, J. Toxicol. Environ. Heal. - Part B Crit. Rev., 2, 1 (1999) 87–104.

[8] J. Dong *et. al.*, Metal-organic frameworks with Tb_4 clusters as nodes: Luminescent

detection of chromium (VI) and chemical fixation of CO_2, Inorg. Chem., 56, 11 (2017) 6244–6250.

[9] H. Chen *et. al.,* Separation and preconcentration system based on ultrasonic probe-assisted ionic liquid dispersive liquid-liquid microextraction for determination trace amount of chromium(VI) by electrothermal atomic absorption spectrometry, Talanta, 81, 1–2 (2010) 176–179.

[10] Y. Miyake *et. al.*, Determination of hexavalent chromium concentration in industrial waste incinerator stack gas by using a modified ion chromatography with post-column derivatization method, J. Chromatogr. A, 1502 (2017) 24–29.

[11] N. Unceta *et. al.*, A novel strategy for Cr (III) and Cr (VI) analysis in dietary supplements by speciated isotope dilution mass spectrometry, Talanta., 154 (2016) 255–262.

[12] X. Bu *et. al.*, Highly sensitive SERS determination of chromium (VI) in water based on carbimazole functionalized alginate-protected silver nanoparticles, Sensors Actuators B. Chem., 273 (2018) 1519–1524.

[13] S. M. Rosolina *et. al.*, Highly sensitive detection of hexavalent chromium utilizing a sol-gel/carbon nanotube modified electrode, J. Electroanal. Chem., 781 (2016) 120–125.

[14] N. A. Carrington *et. al.*, Optical determination of Cr (VI) using regenerable, functionalized sol-gel monoliths, Anal. Chim. Acta., 581, 2 (2007) 232–240.

[15] J. R. Peralta-Videa *et. al.*, Nanomaterials and the environment: A review for the biennium 2008-2010, J. Hazard. Mater., 186, 1 (2011) 1–15.

[16] W. Shi *et. al.*, Carbon nanodots as peroxidase mimetics and their applications to glucose detection, Chem. Commun.,. 47, 23 (2011) 6695–6697.

[17] C. Ren, X. Hu, and Q. Zhou, Graphene oxide quantum dots reduce oxidative stress and inhibit neurotoxicity in- vitro and in- vivo through catalase- like activity and metabolic regulation, Adv. Sci., 5, 5 (2018) 1700595.

[18] L. Gao *et. al.*, Intrinsic peroxidase-like activity of ferromagnetic nanoparticles, Nat. Nanotechnol., 2, 9 (2007) 577–583.

[19] V. Baldim *et. al.*, The enzyme-like catalytic activity of cerium oxide nanoparticles and its dependency on Ce^{3+} surface area concentration, Nanoscale., 10, 15 (2018) 6971–6980.

[20] L. Yong- Ge *et. al.*, Morphology-controlled synthesis of Co_3O_4 nanocubes and their catalytic performance in CO oxidation, Acta. Phys. Chim. Sin., 30, 2 (2014) 382–388.

[21] A. R. Wassel *et. al.*, Recent advances in polymer/metal/metal oxide hybrid nanostructures for catalytic applications: A review, J. Environ. Chem. Eng., 8, 5 (2020) 104175.

[22] F. Paquin *et. al.*, Multi-phase semicrystalline microstructures drive exciton dissociation in neat plastic semiconductors," J. Mater. Chem. C., 3 (2015) 10715–10722.

[23] M. Serhan *et. al.*, Total iron measurement in human serum with a smartphone," AIChE Annu. Meet. Conf. Proc., (2019) doi: 10.1039/x0xx00000x.

[24] A. De La Escosura-Muñiz *et. al.*, Immunosensing using nanoparticles, Mater. Today., 13, 7–8 (2010) 24–34.

[25] W. Yang *et. al.*, Nanozymes: Activity origin, catalytic mechanism, and biological application, Coord. Chem. Rev., 448 (2021) 214170.

[26] S. Dubchak *et. al.*, Influence of silver and titanium nanoparticles on arbuscular mycorrhiza colonization and accumulation of radiocaesium in Helianthus annuus, Spanish J. Agric. Res., 8 (2010) 103–108.

[27] C. Y. Wu, Nanoparticles and the environment, J. Air Waste Manag. Assoc., 55, 6 (2005) 708–746.

[28] E. L. S. Wong *et. al.*, Nanozymes for environmental pollutant monitoring and remediation, Sensors (Switzerland)., 21, 2 (2021) 1–47.

[29] X. Wu *et. al.*, Modified Ti_3C_2 nanosheets as peroxidase mimetics for use in colorimetric detection and immunoassays, J. Mater. Chem. B., 8, 13 (2020) 2650–2659.

[30] Y. Song *et. al.*, Graphene oxide: Intrinsic peroxidase catalytic activity and its application to glucose detection, Adv. Mater., 22, 19 (2010) 2206–2210.

[31] A. A. Vernekar *et. al.*, An antioxidant nanozyme that uncovers the cytoprotective potential of vanadia nanowires, Nat. Commun., 5 (2014) 6301.

[32] Y. Jv *et. al.,* Positively-charged gold nanoparticles as peroxidiase mimic and their application in hydrogen peroxide and glucose detection, Chem. Commun., 46, 42 (2010) 8017–8019.

[33] W. Chen *et. al.,* Peroxidase-like activity of cupric oxide nanoparticle, ChemCatChem., 3, 7 (2011) 1151–1154.

[34] B. Garg and T. Bisht, Carbon nanodots as peroxidase nanozymes for biosensing, Molecules., 21, 12 (2016) 1–16.

[35] L. Chang *et. al.,* Multifunctional janus hematite-silica nanoparticles: mimicking peroxidase-like activity and sensitive colorimetric detection of glucose, ACS. Appl. Matter. Interfaces., (2015), doi: 10.1021/acsami.5b03423.

[36] M. T. Alula and K. Feke, Peroxidase-like activity of silver nanoparticles loaded filter paper and its potential application for sensing, J. Clust. Sci., 5 (2021).

[37] C. Jiang *et. al.,* A colorimetric sensor based on Glutathione-AgNPs as peroxidase mimetics for the sensitive detection of Thiamine (Vitamin B1), Spectrochim. Acta Part A Mol. Biomol. Spectrosc., 265 (2022) 120348.

[38] Y. Wang *et. al.,* Enzyme kinetics by isothermal titration calorimetry: Allostery, inhibition, and dynamics, Front. Mol. Biosci., 7 (2020) 1–19.

[39] W. W. Cleland, Derivation of rate equations for multisite ping pong mechanisms with ping pong reactions at one or more sites, J. Biol. Chem., 248, 24 (1973) 8353–8355.

[40] Y. Chong *et. al.,* Advances in oxidase-mimicking nanozymes: Classification, activity regulation and biomedical applications, Nano Today., 37 (2021) 101076.

[41] A. Asati *et. al.,* Oxidase-like activity of polymer- coated cerium oxide, Angew. Chem., 121, (2009) 2344–2348.

[42] L. Guo *et. al.*, Biocompatibility selenium nanoparticles with an intrinsic oxidase-like activity, J. Nanoparticle Res., 18, 3 (2016) 1–10.

[43] Q. Cheng *et. al.,* Pt nanoparticles with high oxidase-like activity and reusability for detection of ascorbic acid, Nanomaterials.,10 (2020) 1015.

[44] T. Pirmohamed *et al.,* Nanoceria exhibit redox state-dependent catalase mimetic activity, Chem. Commun., 46, 16 (2010) 2736–2738.

[45] R. Singh and S. Singh, Role of phosphate on stability and catalase mimetic activity of cerium oxide nanoparticles, Colloids Surfaces B Biointerfaces., 132 (2015) 78–84.

[46] S. S. Ali *et al.,* A biologically effective fullerene (C_{60}) derivative with superoxide dismutase mimetic properties, Free Radic. Biol. Med., 37, 8 (2004) 1191–1202.

[47] D. Wang *et. al.,* AuNPs@NC@MnO_2 with exceptional nano-enzyme activity for sensitive colorimetric detection of Cr (VI)," Microchem. J., 181 (2022) 107706.

[48] F. Li *et al.,* Non-aggregation based label free colorimetric sensor for the detection of Cr (VI) based on selective etching of gold nanorods, Sensors Actuators B. Chem., 155, 2 (2011) 817–822.

[49] S. Babazadeh *et. al.,* Colorimetric detection of chromium (VI) ions in water using unfolded-fullerene carbon nanoparticles, sensors., 21 (2021) 6353.

[50] J. Guo *et. al.,* Colorimetric detection of Cr (VI) based on the leeching of gold nanoparticles using a paper- based sensor, Talanta., 161 (2016) 819–825.

[51] A. Ravindran *et. al.,* Selective colorimetric detection of nanomolar Cr (VI) in aqueous solutions using unmodified silver nanoparticles, Sensors Actuators B. Chem., 166–167 (2012) 365–371.

[52] N. N. Nghia *et. al.,* Colorimetric detection of chromium (VI) using graphene oxide nanoparticles acting as a peroxidase mimetic catalyst and 8-hydroxyquinoline as an inhibitor, Microchimica. Acta., 186 (2019) 36.

[53] Y. Mao *et. al.,* Single-atom nanozyme enabled fast and highly sensitive colorimetric detection of Cr (VI), J. Hazard. Mater., 408 (2021) 124898.

[54] S. Ghayyem *et. al.*, Colorimetric detection of chromium (VI) ion using poly (N-phenylglycine) nanoparticles acting as a peroxidase mimetic catalyst, Talanta., 226 (2021) 122082.

[55] Y. Qi *et. al.,* Determination of Cr (VI) based on the peroxidase mimetic catalytic activity

of citrate-capped gold nanoparticles, Microchimica. Acta., 188 (2021) 273.

[56] A. Swaidan *et. al.*, A facile preparation of CuS-BSA nanocomposite as enzyme mimics : Application for selective and sensitive sensing of Cr (VI) ions, Sensors Actuators B. Chem., 294 (2019) 253–262.

[57] N. A. Chamaraja *et. al.*, Colorimetric detection of chromium (VI) using peroxidase mimetic IONPS with 4- Aminoantipyrene and 3-Aminophenol as a chromogen, Environ. Nanotechnol. Monit. Manag., 16 (2021) 1–8.

[58] M. T. Alula and M. L. Madingwane, Colorimetric quantification of chromium (VI) ions based on oxidoreductase-like activity of Fe_3O_4, Sens. Actuators B: Chem., 324 (2020) 128726.

[59] Q. Xue *et. al.*, Polyethylenimine-stabilized silver nanoclusters act as an oxidoreductase mimic for colorimetric determination of chromium (VI), Microchim. Acta., 187, 5 (2020) 21–23.

[60] C. A. Kozlowski and W. Walkowiak, Removal of chromium (VI) from aqueous solutions by polymer inclusion membranes, Water Res., 36, 19 (2002) 4870–4876.

[61] N. B. Singh *et. al.*, Water purification by using adsorbents: A Review, Environ. Technol. Innov., 11 (2018) 187–240.

[62] R. Verma, Heavy metal water pollution- A case study, Recent Res. Sci. Technol., 5 (2017) 98–99.

[63] F. D. Owa, Water pollution: Sources, effects, control and management, Mediterr. J. Soc. Sci., 4, 8 (2013) 65–68.

[64] R. Verma and P. Dwivedi, Heavy metal water pollution- A case study, Recent Res. Sci. Technol., 5, 5 (2013) 98–99.

[65] D. Cremean and E. J. Techera, Marine pollution law, Routledge Handb. Int. Environ. Law., 2002 (2012) 277–293.

[66] I. J. El Saliby *et. al.*, Nanotechnology for water treatment: In brief, EOLSS., 1999.

[67] R. H. Meade, Contaminants in the Mississippi River, | 1987-92, Government Printing.,

1133 (1987).

[68] World Health Organization, Safety evaluation of certain contaminants in food, JECFA., (1002) 2017.

[69] X. Qu *et. al.,* Applications of nanotechnology in water and wastewater treatment, Water Res., 47, 12 (2013) 3931–3946.

[70] I. Tlili and T. A. Alkanhal, Nanotechnology for water purification: Electrospun nanofibrous membrane in water and wastewater treatment, J. Water Reuse Desalin., 9, 3 (2019) 232–247.

[71] N. Morin *et. al.*, Worldwide cases of water pollution by emerging contaminants: a review, 2020, doi.org/10.1007/s10311-022-01447-4.

[72] U. Pradesh *et. al.*, Emerging pollutants in aquatic environment :Source, effect and challenges in biomonitoring and bioremediation- A review, Pollution., 6, 1 (2020) 99–113.

[73] N. Z. Arman *et. al.,* A review on emerging pollutants in the water environment: Existences, health effects and treatment processes, Water., 13, 3258 (2021) 1–31.

[74] M. Grassi *et. al.*, Removal of emerging contaminants from water and wastewater by adsorption process, SpringerBriefs in Green Chemistry for Sustainability., (2012) 15–37.

[75] F. Fern and A. J. Dos, Degradation of contaminants of emerging concern by electrochemical oxidation: Coupling of ultraviolet and ultrasound radiations, Materials., 16, 5551 (2020).

[76] J. Lund Schlamovitz and P. Becker, Differentiated vulnerabilities and capacities for adaptation to water shortage in Gaborone, Botswana, Int. J. Water Resour. Dev.,37, 2 (2021) 278–299.

[77] S. K. Dickin *et. al.,* A review of health risks and pathways for exposure to wastewater use in agriculture, Environ. Health Perspect., 124, 7 (2016) 900–909.

[78] World Bank, Botswana climate variability and change: Understanding the risks, (2010) 1–56.

[79] B.F. Alemaw *et. al.,* Assessment of ground water pollution vulnerability and modelling of

the Kanye wellfield in SE Botswana: A GIS approach, Physics and Chemistry of the earth., 29 (2004) 1125- 1128.

[80] J. K. Kiptoo *et. al.*, Comparative studies of the speciation patterns of nickel and chromium in surface-, ground- and wastewater systems in Botswana, South African J. Chem., 58, (2005) 120–126.

[81] A. A. Adekanmi, An Investigation of chromium and nickel uptake in tomato plants irrigated with treated waste water at the Glen valley farm, Gaborone, Botswana, (2010).

[82] P. Zhang *et. al.*, Surface plasmon resonance for water pollutant detection and water process analysis, TrAC - Trends Anal. Chem., 85 (2016) 153–165.

[83] Y. W. Fen *et. al.*, Development of surface plasmon resonance sensor for determining zinc ion using novel active nanolayers as probe, Spectrochim. Acta - Part A Mol. Biomol. Spectrosc., 134 (2015) 48–52.

[84] P. C. Pinheiro *et. al.*, Functionalized inorganic nanoparticles for magnetic separation and SERS detection of water pollutants, Eur. J. Inorg. Chem., 2018, 30 (2018) 3443–3461.

[85] J. A. Buledi *et. al.*, A review on detection of heavy metals from aqueous media using nanomaterial-based sensors, Environ. Sci. Pollut. Res., 28, 42 (2021) 58994–59002.

[86] N. Ullah *et. al.*, Nanomaterial-based optical chemical sensors for the detection of heavy metals in water: Recent advances and challenges, TrAC - Trends Anal. Chem., 100 (2018) 155–166.

[87] A. Waheed *et. al.*, Nanomaterials-based electrochemical detection of heavy metals in water: Current status, challenges and future direction, TrAC - Trends Anal. Chem., 105 (2018) 37–51.

[88] A. G. Ferrari *et. al.*, Electroanalytical overview: The detection of chromium, Sensors and Actuators Reports., 4 (2022) 100116.

[89] D. Spanu *et. al.*, One-minute highly selective Cr (VI) determination at ultra-trace levels: An ICP-MS method based on the on-line trapping of Cr (III), J. Hazard. Mater., 412, (2021) 125280.

[90] M. Marcinkowska *et. al.,* Study on multielemental speciation analysis of Cr (VI), As (III) and As (V) in water by advanced hyphenated technique HPLC/ ICP-DRC-MS. Fast and reliable procedures, 144 (2015) 233–240.

[91] W. Zou *et. al.,* Selective determination of Cr (VI) and non-chromatographic speciation analysis of inorganic chromium by chemical vapor generation-inductively coupled plasma mass spectrometry, Talanta, 218 (2020) 121128.

[92] J. Chwastowska *et. al.,* Speciation of chromium in mineral waters and salinas by solid-phase extraction and graphite furnace atomic absorption spectrometry, Talanta., 66, 5 (2005) 1345–1349.

[93] Y. Martínez-Bravo *et. al.,* Multielemental determination of arsenic, selenium and chromium (VI) species in water by high-performance liquid chromatography-inductively coupled plasma mass spectrometry, J. Chromatogr. A., 926, 2 (2001) 265–274.

[94] J. Sun *et. al.,* Simultaneous speciation and determination of arsenic, chromium and cadmium in water samples by high performance liquid chromatography with inductively coupled plasma mass spectrometry, Anal. Methods., 7, 6 (2015) 2653–2658.

[95] M. A. Zaitoun, Spectrophotometric determination of Chromium (VI) using cyclam as a reagent, Int. J. Environ. Anal. Chem., 85, 6 (2005) 399–407.

[96] X. Bu *et. al.,* Highly sensitive SERS determination of chromium (VI) in water based on carbimazole functionalized alginate-protected silver nanoparticles, Sensors Actuators, B Chem., 273 (2018) 1519–1524.

[97] L. Zhou *et al.,* Ag nanoparticles decorated Ag@ZrO_2 composite nanospheres as highly active SERS substrates for quantitative detection of hexavalent chromium in waste water, J. Mol. Liq., 319 (2020) 114158.

[98] D. Dong and C. Zhao, Limitations and challenges of using raman spectroscopy to detect the abiotic plant stress response, Proc. Natl. Acad. Sci. U. S. A., 114, 28 (2017) E5486–E5487.

[99] K. Shrivas *et. al.,* Localized surface plasmon resonance of silver nanoparticles for sensitive colorimetric detection of chromium in surface water, industrial waste water and

vegetable samples, Anal. Methods., 8, 9 (2016) 2088–2096.

[100] K. J. Fahnestock *et. al.*, Selective detection of hexachromium ions by localized surface plasmon resonance measurements using gold nanoparticles/chitosan composite interfaces, Analyst., 134, 5 (2009) 881–886.

[101] A. P. Ingle *et. al.*, Bioactivity, mechanism of action, and cytotoxicity of copper-based nanoparticles: A review, Appl. Microbiol. Biotechnol., 98, 3 (2014) 1001–1009.

[102] M. B. Gawande *et. al.*, Cu and Cu-based nanoparticles: Synthesis and applications in catalysis, Chem. Rev., 116, 6 (2016) 3722–3811.

[103] A. Ahmed *et. al*., Size- and phase- dependent structure of copper (II) oxide nanoparticles, RSV Adv., 5 (2015) 35033- 35041

[104] J. Lai *et. al.*, Solvothermal synthesis of metal nanocrystals and their applications, Nano Today., 10, 2 (2015) 240–267.

[105] Y. Yang *et. al.*, Solvothermal synthesis of platinum nanoparticles and their SERS properties, 5th Int. Symp. Adv. Opt. Manuf. Test. Technol. Optoelectron. Mater. Devices Detect. Imager, Display, Energy Convers. Technol., 7658 (2010) 76580H.

[106] C. Pellerin and S. M. Booker, Reflections on hexavalent chromium, Environmental Health Perspectives., 108, 9 (2000) 402–407.

[107] M. A. Armienta *et. al.*, Chromium in a tannery wastewater irrigated Area, Leon Valley, Mexico, Env. Cont. and Toxicol., 66 (2001) 189–195.

[108] R. K. S. Ingh *et. al.*, Identification and mapping of chromium (VI) plume in groundwater for remediation : A case study at Kanpur, Uttar Pradesh, Geol. Soc. India., 74 (2009) 49–57.

[109] Y. Liu and X. Wang, Colorimetric speciation of Cr(III) and Cr(VI) with a gold nanoparticle probe, Anal. Methods., 5, 6 (2013) 1442–1448.

[110] G. Dönmez and Z. Aksu, Removal of chromium (VI) from saline wastewaters by Dunaliella species, Process Biochem., 38, 5 (2002) 751–762.

[111] M. Zhong *et. al.*, Dual responsive enzyme mimicking of ternary polyaniline-MnO_2-Pd

nanowires and its application in colorimetric biosensing, ACS Sustain. Chem. Eng., 6, 12 (2018) 16482–16492.

[112] W. Cheng *et. al.,* One-step synthesis of superparamagnetic monodisperse porous Fe_3O_4 hollow and core-shell spheres, J. Mater. Chem., 20, 9 (2010) 1799–1805.

[113] Y. Li *et. al.,* Copper sulfide nanoparticles for photothermal ablation of tumor cells, Nanomedicine., 5, 8 (2010) 1161–1171.

[114] X. Zhang *et al.,* Ultrahigh selective colorimetric quantification of chromium (VI) ions based on gold amalgam catalyst oxidoreductase-like activity in water, Anal. Chem., 90, 24 (2018) 14309–14315.

[115] S. K. Li *et al.,* Magnetic Fe_3O_4@C@Cu_2O composites with bean-like core/shell nanostructures: Synthesis, properties and application in recyclable photocatalytic degradation of dye pollutants, J. Mater. Chem., 21, 20 (2011) 7459–7466.

[116] M. Dakiky *et. al.,* Selective adsorption of Cr (VI) in industrial adsorbents, Adv. Environ. Res., 6 (2002) 533–540.

[117] J. F. Amaku *et. al.,* Enhanced sequestration of Cr (VI) onto plant extract anchored on carbon-coated aluminium oxide composite, Environ. Sci. Pollut. Res., 28, 41 (2021) 57723–57738.

[118] P. B. Vilela *et. al.,* Adsorption and removal of chromium (VI) contained in aqueous solutions using a chitosan-based hydrogel, Environ. Sci. Pollut. Res., 26, 28 (2019) (28481-28489.

[119] J. Ma *et. al.,* On-line separation and preconcentration of hexavalent chromium on a novel mesoporous silica adsorbent with determination by solution- cathode glow dischargeatomic emission spectrometry, JAAS., 29, 12 (2014) 2315-2322.

[120] Á. Béni *et.al.,* Separation/ preconcentration of chromium species with continuous liquid-liquid extraction device and its determination by AAS, Microchem. J., 150 (2019) 104077.

[121] S. Mishra *et. al.,* Recent advances in silver nanozymes: Concept, mechanism, and applications in detection, Adv. Mater. Interfaces., 2200928 (2022) 1–18.

[122] J. S. Algethami, A review on recent progress in organic fluorimetric and colorimetric chemosensors for the detection of $Cr^{3+/6+}$ Ions, Crit. Rev. Anal. Chem., 0, 0 (2022) 1–21.

[123] Y. Zhang *et al.*, Highly selective and sensitive probes for the detection of Cr (VI) in aqueous solutions using diglycolic acid-functionalized Au nanoparticles, RSC Adv., 9, 19 (2019) 10958–10965.

[124] C. Dong *et al.*, Selective colorimetric detection of Cr (III) and Cr (VI) using gallic acid 2 capped gold nanoparticles, Dalton Trans., 45, 20 (2016) 8347- 8354.

[125] L. Liu *et. al.*, Photometric and visual detection of Cr (VI) using gold nanoparticles modified with 1,5-diphenylcarbazide, Microchim. Acta., 183, 4 (2016) 1367–1373.

[126] S. He *et. al.*, Colorimetric detection of Cr (VI) using silver nanoparticles functionalized with PVP, Anal. Methods, 11, 45 (2019) 5819–5825.

[127] P. Das *et. al.*, Peroxidase mimic activity of Au-Ag/l-Cys-rGO nanozyme toward detection of Cr (VI) ion in water: Role of 3,3′,5,5′-tetramethylbenzidine adsorption, J. Chem. Eng. Data., 64, 11 (2019) 4977–4990.

[128] M. T. Alula *et. al.*, Biosynthesis of bifunctional silver nanoparticles for catalytic reduction of organic pollutants and optical monitoring of mercury (II) ions using their oxidase-mimic activity, Environ. Sci. Pollut. Res., 29 (2022) 81938-81953.

[129] L. Xiao *et. al.*, Colorimetric biosensor for detection of cancer biomarker by Au nanoparticle-decorated Bi_2Se_3 nanosheets, ACS Appl. Mater. Interfaces., 9, 8 (2017) 6931–6940.

[130] A. Hyder *et. al.*, Identification of heavy metal ions from aqueous environment through gold, silver and copper nanoparticles: An excellent colorimetric approach, Environ. Res., 205 (2022) 112475.

[131] M. T. Alula *et. al.*, Determination of cysteine via its inhibition of catalytic activity of silver coated ZnO/Fe_3O_4 composites used for conversion of 4-nitrophenol into 4-aminophenol, Microchem. J., 156 (2020) 104976.

[132] L. Zheng *et al.*, Recent progress in the construction and applications of metal-organic

frameworks and covalent-organic frameworks-based nanozymes, Coord. Chem. Rev., 471 (2022) 214760.

[133] Q. Wang *et. al.*, Nanozyme: An emerging alternative to natural enzyme for biosensing and immunoassay, TrAC - Trends Anal. Chem., 105 (2018) 218–224.

[134] B. Unnikrishnan *et. al.,* A review on metal nanozyme-based sensing of heavy metal ions: Challenges and future perspectives, J. Hazard. Mater., 401 (2021) 123397.

[135] S. B. He *et. al.,* One-pot cascade catalysis at neutral pH driven by CuO tandem nanozyme for ascorbic acid and alkaline phosphatase detection, Sensors Actuators, B Chem., 321 (2020) 128511.

[136] W. Chen *et. al.*, Peroxidase-like activity of water-soluble cupric oxide nanoparticles and its analytical application for detection of hydrogen peroxide and glucose, Analyst., 137, 7 (2012) 1706–1712.

[137] W. J. Lin *et. al.*, Electrocatalytic CuBr@CuO nanoparticles based salivary glucose probes, Biosens. Bioelectron., 194 (2021) 113610.

[138] Z. Wang *et. al.,* One-step solvothermal synthesis of Fe_3O_4@Cu@Cu_2O nanocomposite as magnetically recyclable mimetic peroxidase, J. Alloys Compd., 682 (2016) 432–440.

[139] S. Jadhav *et. al.,* Copper oxide nanoparticles: Synthesis, characterization and their antibacterial activity, J. Clust. Sci., 22, 2 (2011) 121–129.

[140] M. Kasiri and M. Rahaie, A visible and colorimetric nanobiosensor based on DNA-CuO nanoparticle for detection of single nucleotide polymorphism involved in sickle cell anemia disease, Mater. Today Commun., 27 (2021) 102423.

[141] S. Ali *et. al.*, Synthesis of β-cyclodextrin grafted rhombohedral-CuO antioxidant nanozyme for detection of dopamine and hexavalent chromium through off–on strategy of peroxidase mimicking activity, Microchem. J., 179 (2022) 107514.

[142] J. Cao *et. al.,* Preparation, characterization and visible-light photocatalytic activity of AgI/AgCl/TiO_2, Appl. Surf. Sci., 257, 16 (2011) 7083–7089.

[143] G. Wang *et. al.*, Label-free colorimetric sensor for mercury (II) and DNA on the basis of

mercury (II) switched-on the oxidase-mimicking activity of silver nanoclusters, Anal. Chim. Acta, 871 (2015) 1–8.

[144] Y. Wang *et. al.*, Nanoceria-templated metal organic frameworks with oxidase-mimicking activity boosted by hexavalent chromium, Anal. Chem., 92, 2 (2020) 2339–2346.